# Elucidating the mechanisms of atmospheric new particle formation in the highly polluted Po Valley, Italy

Jing Cai[1], Juha Sulo[1], Yifang Gu[1], Sebastian Holm[1], Runlong Cai[1], Steven Thomas[1], Almuth Neuberger[2], Fredrik Mattsson[2], Marco Paglione[3], Stefano Decesari[3], Matteo Rinaldi[3], Rujing Yin[1], Diego Aliaga[1], Wei Huang[1], Yuanyuan Li[1,4], Yvette Gramlich[2], Giancarlo Ciarelli[1], Lauriane Quéléver[1], Nina Sarnela[1], Katrianne Lehtipalo[1,5], Nora Zannoni[3], Cheng Wu[6], Wei Nie[4], Juha Kangasluoma[1], Claudia Mohr[7,8], Markku Kulmala[1,4,9], Qiaozhi Zha[1,4], Dominik Stolzenburg[1,10*], Federico Bianchi[1*]

[1] Institute for Atmospheric and Earth System Research, Faculty of Science, University of Helsinki, Helsinki 00014, Finland

[2] Department of Environmental Science, Stockholm University, Stockholm 11418, Sweden

[3] Italian National Research Council-Institute of Atmospheric Sciences and Climate (CNR-ISAC), Bologna, 40129, Italy

[4] School of Atmospheric Sciences, Nanjing University, Nanjing, 210023, China

[5] Finnish Meteorological Institute, Helsinki, 00560, Finland

[6] Department of Chemistry and Molecular Biology, Atmospheric Science, University of Gothenburg, Gothenburg 41296, Sweden

[7] Laboratory of Atmospheric Chemistry, Paul Scherrer Institute, Villigen, 5232, Switzerland

[8] Department of Environmental System Science, ETH Zurich, Zurich, 5232, Switzerland

[9] Beijing Advanced Innovation Center for Soft Matter Science and Engineering, Beijing University of Chemical Technology, Beijing 100029, China

[10] Institute for Materials Chemistry, TU Wien, Vienna 1060, Austria

*Correspondence to:* federico.bianchi@helsinki.fi and dominik.stolzenburg@tuwien.ac.at

## Abstract

New particle formation (NPF) is a major source of aerosol particles and cloud condensation nuclei in the troposphere, playing an important role in both air quality and climate. Frequent NPF events have been observed in heavily polluted urban environments, contributing to the aerosol number concentration by a significant amount. The Po Valley region in northern Italy has been characterized as a hotspot for high aerosol loadings and frequent NPF events in Southern Europe. However, the mechanisms of NPF and growth in this region are not completely understood. In this study, we conducted a continuous 2-month measurement campaign with state-of-the-art instruments to elucidate the NPF and the growth mechanisms in Northern Italy. Our results demonstrate that in this area, frequent NPF events (66% of all days during the measurement campaign) are primarily driven by abundant sulfuric acid ($8.5\times10^6$ $cm^{-3}$) and basic molecules. In contrast, oxygenated organic molecules from the atmospheric oxidation of

volatile organic compounds (VOCs) appear to play a minor role in the initial cluster formation but contribute significantly to the consecutive growth process. Regarding alkaline molecules, amines, are insufficient to stabilize all sulfuric acid clusters in Po Valley. Ion cluster measurements and kinetic models suggest that ammonia (10 ppb) must therefore also play a role in the nucleation process. Generally, the high formation rates of sub-2 nm particles (87 $cm^{-3}\,s^{-1}$) and nucleation mode growth rates (5.1 nm $h^{-1}$) together with the relatively low condensational sink ($8.9\times10^{-3}$ $s^{-1}$) will result in a high survival probability of newly formed particles, making NPF crucial for the springtime aerosol number budget. Our results also indicate that reducing key pollutants such as $SO_2$, amine and $NH_3$, could help to decrease the particle number concentrations substantially in the Po Valley region.

## 1. Introduction

New particle formation (NPF) occurs ubiquitously in the troposphere and affects the global climate (Dunne et al., 2016) and local or regional air quality (Kulmala et al., 2021). NPF and further growth of the newly formed particles dominate aerosol number concentrations and are the major contributor to the ultrafine (<100 nm) aerosol budget, which poses a significant health threat to the population in polluted areas (Schraufnagel, 2020). While air pollution mitigation strategies mostly focus on reducing particulate mass (particulate matter below 2.5 μm ($PM_{2.5}$)), ultrafine particle number concentrations might not be affected by such policies (De Jesus et al., 2019). It is therefore essential that we understand the mechanisms leading to NPF in polluted environments to design better targeted air quality strategies for polluted European regions, where $PM_{2.5}$ reduction measures are already implemented.

NPF is closely linked to atmospheric air pollution. Efficient nucleation and growth are crucial factors contributing to haze formation, according for over 65% of the particle number concentrations in urban environment (Kulmala et al., 2021; Guo et al., 2014; Chu et al., 2019; Sebastian et al., 2022). Strong and frequent NPF events have been reported in the most urbanization areas in China, such as the North China Plain (Wang et al., 2015; Wang et al., 2013; Wu et al., 2011; Wu et al., 2007; Shen et al., 2011), Yangtze River Delta (Dai et al., 2017; Yu et al., 2016; Xiao et al., 2015) and Peal River Delta (Yue et al., 2013; Peng et al., 2014; Liu et al., 2008). This observation contradicts theoretical calculations that suggest NPF events are less likely to occur in polluted areas, where high levels of preexisting aerosols acting as condensational sinks (CS) are capable of quickly scavenging gaseous precursors of NPF (Kulmala et al., 2017).

The elucidation of NPF precursors and mechanisms has varied among different sampling locations and studies. No uniform theory or mechanism can elucidate the NPF occurrence in different polluted areas or in different seasons. For example, in Shanghai and Beijing, China, sulfuric acid (SA, $H_2SO_4$) and amines were identified as key contributors to initial particle formations (Yao et al., 2018; Cai et al., 2021; Yan et al., 2021). On the other hand, some studies also suggests that photooxidation products of vehicle emitted organic vapors, dominate NPF in urban conditions rather than SA or base species (Guo et al., 2020). Meanwhile, in Barcelona, Spain, which is significantly less polluted than Asian megacities but still shows frequent high pollution levels, NPF was reported to be associated with SA along with highly oxygenated organic molecules (HOMs) (Brean et al., 2020). The discrepancies in the reported NPF mechanisms may arise from the limited utilization of state-of-the-art instruments, such as those capable of measuring size distribution down to 1-2 nm and directly identifying clusters and vapors with the influences by spatio-temporal variations (Wang et al., 2017). Therefore, gaining a better knowledge of the key participants, nucleation mechanism and the roles of pre-existing particles is crucial for comprehending the causes of the high NPF frequencies in polluted regions. This knowledge can be essential for developing effective local $PM_{2.5}$ control and implementation strategies.

The Po Valley region is one of the most important industrial and agricultural areas in Southern Europe with dense population (>17 million/70,000 $km^2$). It is located in northern Italy, surrounded by the Alps (in the north), the Apennine mountains (in the south), and the Adriatic Sea (in the east). High primary anthropogenic emissions, a mixture of numerous pollutants from industrial, urban and agricultural sources, together with frequently occurring stagnant meteorological conditions in winter make the Po

Valley region a hotspot in Europe for high aerosol loadings (Saarikoski et al., 2012; Li et al., 2014; Finzi and Tebaldi, 1982; Daellenbach et al., 2023). But it is distinct from Asian megacities as the population density is significantly lower (250 people $km^{-2}$ in Po Valley compared to e.g., 1,400 people $km^{-2}$ in Beijing), resulting in effects such as traffic or residential heating being less dominant pollution sources. At the same time, NPF occurs frequently in the Po Valley (Hamed et al., 2007; Manninen et al., 2010). For example, Shen et al. (2021) observed that NPF events took place on approximately 70% of the days during spring and summer. Similarly, Kontkanen et al. (2017) discovered that during summer, NPF occurred on 89% of the days. During NPF event days, high formation rates of sub-2nm neutral particles ($J_2$, ~$10^1$ to $10^2$ $cm^{-3}$ $s^{-1}$, (Kontkanen et al., 2017)) and SA concentrations (~$1\times10^7$ $cm^{-3}$) were observed in the Po Valley (Paasonen et al., 2010; Kontkanen et al., 2017). These levels were among the highest recorded in a study conducted at nine sites across the Northern Hemisphere (Kontkanen et al., 2017).

While previous studies conducted in the Po Valley have reported frequent NPF events characterized by high nucleation and growth rates, the clustering mechanism and the dominant precursors for particle growth have not been investigated to-date. Especially with respect to the distinct features of Po-Valley compared to the more intensely researched megacity environments, a deeper understanding of frequent NPF events, including their precursors, nucleation mechanisms, and growth processes is crucial for air pollution control and the effective implementation of $PM_{2.5}$ mitigation measures in such a semi-urban but highly industrialized region. In this study, we conducted a 2-month field campaign in the months of March – April 2022, we 1) identified the chemical composition of atmospheric neutral and ion clusters by a set of state-of-the-art mass spectrometers, 2) characterized the initial NPF and further growth rates using particle number size distribution measurement down to 1 nm, and 3) compared the field measurement results with the recent Cosmics Leaving Outdoor Droplets (CLOUD) chamber experiments to investigate the mechanism of NPF events in the Po Valley region. This allowed us to elucidate the NPF and growth mechanisms at a polluted Southern European site, and to give insights in best mitigation strategies for ultrafine particle pollution in the context of already implemented $PM_{2.5}$ reduction strategies.

## 2. Method

### 2.1 Measurement site

Our measurement was part of the Fog and Aerosol InterRAction Research Italy (FAIRARI) field campaign in San Pietro Capofiume (SPC, 44.65°N, 11.62°E, 5 m a.s.l.), located in the Po Valley region in Northern Italy. The measurement site is part of the Aerosol, Clouds and Trace Gases Research Infrastructure (ACTRIS)-Italy network and operated by the Italian National Research Council-Institute of Atmospheric Sciences and Climate (CNR-ISAC). The SPC site is approximately 30 km northeast of Bologna (~400, 000 residents) and 20 km south of Ferrara (~130, 000 residents), the two major cities in the area. The distance from the measurement site to the Adriatic Sea (to the east) is about 50 km. The area around the sampling site consists of agricultural fields, a smaller town (<2, 000 inhabitants, within 5 km) and smaller settlements in the proximity. Given its location, the SPC rural station is considered to be representative of the regional background of the Po Valley (Paglione et al., 2021; Paasonen et al., 2010; Hamed et al., 2007; Saarikoski et al., 2012; Decesari et al., 2014; Paglione et al., 2020). The instruments for the NPF measurement were operated in a temperature controlled (~20 °C) container from March 1 to April 30, 2022.

During the sampling period, the daily average temperature ranged from 1°C to 17°C. The average wind speed (WS) was approximately 2.4±1.5 m/s (Fig. 1b). The average WS in the daytime was 3.5 m/s from the east, which was significantly higher than at night (1.5 m/s) from the west. Strong diurnal variations of wind direction were observed, which was typically from the west at night and shifted to the east during the day (Fig. 1a). This pattern was potentially influenced by the sea-land breeze from the Adriatic Sea. Accordingly, the daily average relative humidity (RH) varied from 41% to 98%, with values as

high as 85% at night, which sharply decreased to around 40% at noon caused by the strong temperature variation.

## 2.2 Instruments

### 2.2.1 Chemical composition measurements

The chemical composition of cluster ions was measured using a high-resolution atmospheric-pressure-interface time-of-flight mass spectrometer (APi-TOF, Aerodyne Research Inc. & Tofwerk AG). The APi-TOF measures naturally charged ions in the ambient environment. A detailed description of the instrument can be found in Junninen et al. (2010). In this study, ambient air was sampled through a 0.57-meter stainless steel tube with a flow rate of ~10 liters per minute (LPM), with 0.8 LPM of the sample flow entering the APi-TOF.

The concentration of SA was measured using a nitrate ion ($NO_3^-$)-based chemical-ionization (CI) atmospheric-pressure-interface time-of-flight mass spectrometer (CI-APi-TOF, Aerodyne Research Inc. & Tofwerk AG (Jokinen et al., 2012)). The CI-APi-TOF is an APi-TOF coupled with a CI-unit, equipped with a soft X-ray source (L9490, Hamamatsu's 9.5 kV) to produce the primary ions. The sampling flow went into the instrument through a ~0.6-meter ¾ inch stainless steel tube. The sampling flow was 10 LPM and the sheath flow was set to 20 LPM. Data acquisitions for CI-APi-TOF was performed with a time resolution of 10 s. A calibration factor of $1.0\times10^{10}$ $cm^{-3}$ for SA was determined with sampling loss corrections before the campaign according to the method proposed by Kurten et al. (2012).

Dimethylamine (DMA) measurements were performed using a Vocus CI-ToF (time-of-flight) mass spectrometer (hereafter Vocus, Aerodyne Research Inc. & Tofwerk AG) using $H_3O^+$ as a reagent ion. The Vocus has been described in detail in Krechmer et al. (2018) and the study by Wang et al. (2020) utilized Vocus for DMA observations. In this study, the Focusing Ion-Molecular Reactor (FIMR) of Vocus operated at a pressure of 2.0 mbar and a temperature of 100 ℃ with the radio frequency amplitude of 350 V and frequency of $1.4 \times 10^6$ Hz. Data acquisition was performed with a time resolution of 10 s in the mass range 0 –1000 amu.

### 2.2.2 Particle size distribution measurements

**Particle Size Magnifier**

The Airmodus A11 nano-CNC-system (nano-Condensation Nucleus Counter), colloquially known as the Particle Size Magnifier (PSM) is a two-step condensation particle counter (CPC) capable of measuring particle size distributions of sub-3nm particles (Vanhanen et al., 2011). The system consists of two parts, in which the PSM (Airmodus A10) acts as a preconditioner where particles are grown first before being funneled to the CPC (Airmodus A20) for further growth and optical detection. In the PSM the sample flow is turbulently mixed with a heated flow saturated with diethylene glycol (DEG) in the mixing section and the DEG then condenses on the particles in the growth tube. By scanning the flow rate through the DEG saturator, the smallest activated particle size is altered which can be converted into a sub-3nm particle size distribution. Further particle growth is achieved by butanol in the CPC such that the particles reach optically detectable sizes.

The PSM was calibrated according to the standard operation procedure for PSM (Lehtipalo et al., 2022) using a known aerosol population from a glowing tungsten wire generator (Kangasluoma et al., 2015; Peineke et al., 2006). The detection efficiency for different particle sizes was determined by comparing the concentration of size selected particles to a reference instrument, in this case a Faraday cup electrometer.

The system was set up with an Airmodus Nanoparticle Diluter (AND) inlet (Lampimäki et al., 2023) for sample dilution and automatic background measurement to make sure that the CPC stays within a single counting range during the campaign. The inlet was set up at around 2 meters above the ground

and the background was measured roughly every 8 hours and subtracted from the signal during the inversion process.

**HFDMPS and Hauke-type DMPS**

The high-flow differential mobility particle sizer (HFDMPS) system utilizes a half-mini differential mobility analyzer (DMA, (Fernández De La Mora and Kozlowski, 2013; Cai et al., 2018)) to size-select particles that are then grown and detected by an A11 nano Condensation Nucleus Counter system (Airmodus Ltd., A11 nano-CNC) (Kangasluoma et al., 2018). The HFDMPS significantly improves sub-10 nm particle measurements compared to a typical differential mobility particle sizer (DMPS) system, allowing us to better characterize the sub-10 nm particle size distribution when combined with the PSM measurements. The DMA was size-calibrated with electro sprayed positively charged monomer ions of tetraheptylammonium bromide (THA+) (Ude and De La Mora, 2005).

The HFDMPS inlet was set up at a height of 1 m and used a 50 cm long 10 mm outer diameter tube with a core sampling system to minimize losses (Kangasluoma et al., 2016; Fu et al., 2019). A home-built Soft X-Ray ionization source (similar to the TSI Inc. Model 3087) was used to charge particles. The HFDMPS measured the particle size-distribution from 2–15 nm for both polarities at 15 predefined size-steps within 10 minutes.

Sampling from the same inlet and using the same charging device, a conventional DMPS system equipped with a Hauke-type DMA (aerosol flow 1 LPM, sheath flow 5 LPM) and a TSI Inc. CPC (Model 3772) was measuring the particle size-distribution from 10–800 nm at 16 predefined size-steps within 10 minutes. In addition, a DMPS measuring from 15–800 nm was available in another measurement container at the same field site. The total particle number concentrations obtained from integrating the particle size-distribution measured by the DMPS was compared with a reference CPC (TSI Inc. Model 3025A) operated at the same site during the first weeks of the campaign. It revealed on average a factor of 2 lower concentrations measured by the Hauke-type DMPS which was confirmed to be rather size-independent by a comparison of the measured size-distributions and their overlap with the HFDMPS system and was thus subsequently corrected for.

### 2.2.3 Co-located measurements

Additional co-located measurements of auxiliary data from CNR-ISAC network (www.isac.cnr.it/en) and from the routine monitoring program of the Regional environmental protection agency of Emilia Romagna (ARPAE, https://www.arpae.it/it) were used in this study. An online High-Resolution Time-of-Flight Aerosol Mass Spectrometer (HR-ToF-AMS, Aerodyne Research) and a Multi Angle Absorption Photometer (MAAP, Thermo Scientific) were operated on the same site for the measurement of non-refractory species and black carbon (BC), respectively. Trace gases were also measured with 1 minute time resolution: $O_3$ (Thermo Scientific, model TEI-49i), $NO_x$ (Teledyne-API, model 200A), $NH_3$ (Teledyne-API, model 201E), and $SO_2$ (Thermo Scientific, Model 43i Trace Level-Enhanced). Moreover, meteorological parameters (e.g., RH, temperature, wind direction and wind speed) were measured by a meteorology station (VAISALA Ltd, model wxt536).

## 2.3 Data processing

### 2.3.1 New particle formation classification

We classified each day according to whether a growing mode appeared in the particle size distribution or not. This classification was done separately for both the HFDMPS and the PSM data. A growing mode was defined as a new particle mode that appeared in the particle size distribution and continued to grow to larger sizes for at least two hours. If there was a growing mode visible in both the PSM and HFDMPS data, the day was defined as "NPF with growth". If there was no growth or the growth was unclear in the HFDMPS data but there was a growing mode in the PSM data, then the day was classified as “NPF with no growth”. If there was no growing mode in either size distributions measured by HFDMPS and PSM, then the day was marked as "no NPF events" (Fig. S1). The definition is similar to Dada et al. (2018) who used naturally charged ions to separate between NPF days with clustering

only and clustering plus visible growth. If there was a growing or an undefined new mode visible in the combined size distribution but there was no clustering detected by the PSM, this day was marked as "unclear". Days that lacked data from one of the instruments were marked as "no data".

### 2.3.2 Condensation sink, nucleation and growth rate calculations

The condensation sink and coagulation sink were calculated according to Dal Maso et al. (2005) from the Hauke-type DMPS size distribution without any correction of aerosol hygroscopic behavior. Growth rates were calculated using the maximum concentration method, in which we fit a Gaussian distribution to the particle concentration evolution at a fixed size to determine the time of maximum concentration for a given size channel in the HFDMPS.

The growth rates were calculated by first determining the time to reach 50% of the maximum concentration and then the average growth rate is derived as the slope of the linear fit between the time and diameter:

$$GR = \frac{\Delta d_p}{\Delta t} \approx \frac{d_{p,f} - d_{p,i}}{t_f - t_i}, \qquad (1)$$

where $d_{p,f}$ is the diameter at the end time $t_f$ and $d_{p,i}$ is the diameter at the start time $t_i$.

From these, the growth rate was calculated as the slope of a linear least squares fit to the time-points of maximum concentration and their corresponding particle diameters. The formation rates were calculated for several sizes by using the balance equation in Kulmala et al. (2012) using the combined DMPS size-distributions ($J_2$, $J_3$, $J_6$) and the PSM plus combined DMPS size-distribution ($J_{1.7}$). Formation rates were then calculated by rearranging the equation describing the time evolution of the particle size distribution. Formation rate for a given diameter $d_{p1}$ is calculated as

$$J_{dp1} = \frac{dN_{dp1-dp2}}{dt} + CoagS_{dp1} \cdot N_{dp1-dp2} + \frac{GR}{\Delta d_p} N_{dp1-dp2}, \quad (2)$$

### 2.3.3 Mass spectrometer data analysis

The APi-TOF and CI-APi-TOF data were analyzed using the Tofware package (v.3.1.0, Tofwerk, Switzerland, and Aerodyne, USA) in the Igor Pro software (v.7.08, WaveMetrics, USA). The mass accuracy is within 10 ppm (APi-TOF) and 5 ppm (CI-APi-TOF), and the mass resolutions were ~4500 (APi-TOF) and ~5000 (CI-APi-TOF) for ions >200 Th. The raw signals were firstly normalized by the primary ions ($NO_3^-$, monomer, dimer and trimer) and then multiplied by the calibration factor of SA. Detailed information on the mass spectrometer data analysis methods can be found in previous studies (Cai et al., 2022; Cai et al., 2023a; Zha et al., 2018; Zha et al., 2023a; Fan et al., 2021; Zha et al., 2023b).

### 2.3.4 Kinetic model Simulations

In order to evaluate the contribution of SA-amine clustering to cluster formation in the Po Valley, we applied a kinetic model to simulate SA dimer concentrations. We simulated the cluster concentrations and particle formation rates under different amine levels based on the model. The simulation was performed with a temperature of 283 K, atmospheric pressure of $1.01\times10^5$ Pa, and the condensation sink (CS) of 0.01 $s^{-1}$ based on our measurement during the sampling period. In the model, the formation rate of SA tetramer was regarded as the simulated particle formation rate. The standard molar Gibbs free energy of formation and the corresponding evaporation of SA-amine clusters was based on quantum chemistry with corrections from the experimental data. The detailed settings of the kinetic model can be found in Cai et al. (2021).

## 3. Results and discussions

### 3.1 NPF event frequency in Po Valley

During the measurement period, frequent NPF events occurred in Po Valley (Fig. 2, Fig. S1). On 27% of the days, we observed new particle formation with growth at the site, while on 39% of the days we observed new particle formation without growth. In total we observed new sub-3 nm clusters forming on 66 % of the days (Fig. 2). Even though we applied the similar definition of NPF events as previous

study, we can only compare our NPF events with growth type with the reported NPF event frequency due to the lack of capacity to measure the sub-3nm particles in previous literature. Our results were similar to those by Hamed et al. (2007) who observed NPF events on 36 % of the time in March and April of 2002 at the same site. Manninen et al. (2010) observed NPF events during more than half of all days from March to Oct in 2008 and Kontkanen et al. (2016) observed NPF during 89 % of the days in July at the same site, which is higher than our observations. Hamed et al. (2007) also observed that NPF with growth events on 60% of the days during summer, which suggests that summertime NPF frequency at SPC is typically higher than our observation in springtime 2022. This difference in the observed NPF frequency was likely due to the different season with favorable conditions for NPF such as potential lower CS (due to less stagnant meteorological conditions) and higher basic and organic molecule concentrations in summer. In addition, the abundant solar radiation and low aerosol water content (limiting surface area and heterogenous reactions (Du et al., 2022)), likely create favorable conditions for NPF to occur.

The median average particle formation rates at 1.7 nm, 3 nm and 7 nm for all sampling days with NPF with growth events were 87 $cm^{-3}$ $s^{-1}$ (32 – 133 $cm^{-3}$ $s^{-1}$), 3.2 $cm^{-3}$ $s^{-1}$ (1.4 $cm^{-3}$ $s^{-1}$ – 7.0 $cm^{-3}$ $s^{-1}$) and 1.4 $cm^{-3}$ $s^{-1}$ (0.3 $cm^{-3}$ $s^{-1}$ – 3.0 $cm^{-3}$ $s^{-1}$), respectively. The formation rate at 1.7 nm during NPF with growth days (NPF with growth, 87 $cm^{-3}$ $s^{-1}$) is similar to that observed previously at the same site by Kontkanen et al. (2016) in summer. The high formation rate, which is comparable with heavily polluted urban environments such as Beijing and Shanghai, China (59 $cm^{-3}$ $s^{-1}$ – 225 $cm^{-3}$ $s^{-1}$ (Deng et al., 2020; Yao et al., 2018)), will be further discussed in section 3.4. The average formation rate ($J_{1.7}$) on NPF days without growth (24 $cm^{-3}$ $s^{-1}$) is much lower. During the noontime, the formation rate of particles for NPF events with no growth was less than half of $J_{1.7}$ for NPF with growth (Fig. S2). It suggests that for particles to grow in a polluted environment such as the Po Valley, there needs to be abundant clustering to overcome losses to the existing condensation sink so that at least some of the particles survive to grow into larger sizes.

SA has long been known as a primary gaseous precursor for NPF in continental environments, owing to its extremely low volatility (Kirkby et al., 2011; Kulmala et al., 2013). During our sampling period, we observed high SA concentration in the Po Valley, in accordance with the frequent NPF events. The daily average SA concentration measured between 10:00 – 14:00 LT was $4.6\times10^6$ $cm^{-3}$, which increased to $8.5\times10^6$ $cm^{-3}$ during NPF events with growth, aligning with previous findings from the same site ($1.6\times10^7$ $cm^{-3}$ during NPF in summer of 2009, (Paasonen et al., 2010)). Over the entire sampling period (10:00 – 14:00 LT), SA showed a moderately correlation with the calculated $J_{1.7}$ ($r$ = 0.49, Spearman correlation coefficient, for the logarithmic values), but its relationship varied among different days. This suggests that in addition to SA, other components, such as basic molecules, may also contribute to driving NPF events and subsequent growth in the Po Valley.

### 3.2 Nucleation mechanism

To investigate the NPF mechanism in the Po Valley, in this study we firstly compared the simultaneously measured $J_{1.7}$ and SA with recent Cosmics Leaving Outdoor Droplets (CLOUD) chamber experiments that simulated NPF under polluted boundary layer conditions with anthropogenic emissions (Xiao et al., 2021). In those experiments, amines, ammonia, as well as aromatics were added to reflect a heavily anthropogenic emission-influenced environment. Certain basic molecules, including amines (e.g., dimethylamine (DMA)) and ammonia ($NH_3$) have been shown to substantially enhance nucleation and reduce evaporation by stabilizing atmospheric SA in chamber studies (Almeida et al., 2013). Besides, oxygenated organic molecules (OOMs) can also contribute to NPF and subsequent particle growth, even without the inclusion of SA (Kirkby et al., 2016; Xiao et al., 2021). As shown in Fig. 3a, most of the measurements were above the SA-$NH_3$ system at 278K from the CLOUD chamber, suggesting the SA-$NH_3$ mechanism itself cannot solely explain the measured $J_{1.7}$ and that other species are most likely participating to NPF in the Po Valley. For instance, amines, such as DMA or TMA, with higher basicity may contribute to NPF, consistent with not negligible concentrations of amines in

previous studies in the aerosol at SPC (Paglione et al., 2014; Decesari et al., 2014). For the whole sampling period, the median SA and $J_{1.7}$ values in Po Valley follows the SA-DMA-$NH_3$ (4 ppt DMA and 1ppb $NH_3$) and SA-DMA-$NH_3$-Org (adding additional oxidized aromatic organics (Xiao et al., 2021)) lines from the CLOUD chamber at 293K even though during most of the NPF days the average noontime temperature was around 285K (Fig. 3a).

The SA dimer measured by CI-APi-TOF is typically used as an indicator for the initial step for the cluster formation in NPF events (Yan et al., 2021). According to a previous study (Yan et al., 2021), the source and sink terms of the SA dimer can be determined by calculating the formation rate from SA monomer collisions and the loss rate from the SA dimer through coagulation onto pre-existing particles (Fig. 2b). In general, the correlation coefficient between SA dimer and its source to sink term ratios ($r$ = 0.80, Spearman correlation coefficient) indicated that similar to Chinese urban areas, SA dimer was in a pseudo steady-state between the formation of SA monomer collision and the loss onto CS by coagulation.

To further assess the influence of DMA, one of the most common and efficient base molecules for NPF in urban environments (Yao et al., 2018), we compared the measured SA dimer concentrations with the simulated ones under different DMA levels (from 0.1 ppt to reaching kinetic limit) by the kinetic model (Fig. 3b). From our cluster kinetics simulations, during the peak hours of NPF, DMA concentrations are expected to be in the range of 0.1 ppt to 5 ppt, which is lower than the need for reaching the kinetic limit (Figs. 3b and S3). It implies that other factors, for example, the abundant ambient $NH_3$ (~10 ppb) or trimethylamine (TMA) during our study period may also participate in cluster formation. It is consistent with the Vocus measurement, which suggests the ambient DMA signals were close to the background levels (Fig. S4). The reason for not reaching SA-DMA limit during the campaign could be 1) the relatively lower DMA emissions (such as vehicle flows) than Chinese megacities (Ge et al., 2011; Zhu et al., 2022), and 2) the quickly scavenge caused by photolysis and nighttime high RH (85%) (Leng et al., 2015; Yao et al.,2016). Therefore, both of the abundant ambient $NH_3$ concentrations (~10 ppb) and amines likely participated in cluster formation during our study period.

Median particle growth rates (GR) during NPF events for 1.5 – 3 nm, 3 – 7 nm, 7 – 15 nm were 1.3 (1.0– 2.4) nm $h^{-1}$, 4.6 (2.9 – 5.8) nm $h^{-1}$, and 5.1 (3.8 – 8.8) nm $h^{-1}$, respectively. The values in brackets represent the 25$^{th}$ and the 75$^{th}$ percentile of data (Fig. 3c). Growth rates increase with particle diameters, a phenomenon observed in other campaigns around the world as well (Kontkanen et al., 2017, Kulmala et al., 2013)), typically indicative of an increasing organic vapors contribution with size (e.g., Stolzenburg et al. (2018)). The growth rates observed here were similar to those observed by Kontkanen et al. (2016) at SPC in summer (7.2 nm $h^{-1}$ for 7 – 20 nm) and our 1.5 – 3 nm growth rate matches well with Manninen et al. (2010) (1.5 nm $h^{-1}$) during spring in the Po Valley. A comparison to predicted growth rates from sulfuric acid condensation without organics, which was calculated based on kinetic collisions of the measured SA concentrations and the effect of van-der-Waals forces on the collision frequency ((Stolzenburg et al., 2020), Fig. 3c), suggests that sulfuric acid condensation may be on average sufficient for the growth of the smallest clusters. It supports the argument that in the initial steps of NPF and growth in Po Valley sulfuric acid and its stabilizing molecules (likely the bases $NH_3$ and amines) were controlling particle formation. However, for particles to grow beyond 3 nm in size other vapors were needed, which was suggested by the significantly lower contribution of growth by SA (indicated by the green line) than the measured GR for 3 – 7 nm and 7 – 15 nm (Fig. 3c). Those vapors were likely a mixture of organics from anthropogenic and biogenic origins (with the latter emitted at higher rates during summer). We compared the GR during NPF with and without growth events using the method proposed in Kulmala et al. (2022) where the signal was averaged for all classified non-event days and then an appearance time fit was performed for each size channel independently, revealing also a growth pattern. We found no significant difference for the GR in 7 – 15 nm size range in NPF with or without growth days (GR=5.1 nm $h^{-1}$ in NPF with growth days and GR=6.1 nm $h^{-1}$ in NPF without growth days). Considering the similar CS and GR levels for NPF with

and without growth days, the higher formation rates at 1.7 nm (87 $cm^{-3}$ $s^{-1}$) may be a more important factor to surpass the CS. In stable meteorological conditions, a higher formation rate may significantly elevate the possibility of newly formed particles overcome the CS and continuous grow to larger sizes.

### 3.3 Ion and neutral clusters and further particle growth

During the campaign, we observed and identified different types of ion clusters using the APi-TOF, including SA-$NH_3$, SA-Amine, SA-$NH_3$-Amine, SA-$NH_3$-Org during NPF events. In Fig. 4a, we presented the mass defect plot of the naturally charged ion clusters on April 20$^{th}$, when strong NPF events were observed ($J_{1.7}$: 83 $cm^{-3}$ $s^{-1}$). The presence of these clusters was usually in conjunction with SA tetramers ($SA_4$), pentamers ($SA_5$), and hexamers ($SA_6$), which potentially contribute to the NPF events. In Api-TOF measurement, the absence of basic species in the smallest sulfuric acid clusters is likely attributed to the loss of base molecules within the mass spectrometer (Cai et al., 2022b; Zha et al., 2023; Alfaouri et al., 2022).

Among all SA-base (SA-B) clusters, the most abundant SA-$NH_3$ clusters were from $SA_4$-B to $SA_6$-B (Fig. 4a), even though they are reported to be more easily evaporated than DMA clusters due to collision-induced dissociation (Passananti et al., 2019). Pure SA-Amine clusters were only found in the $SA_4$-B clusters with different types of amines, including methylamine ($C_1$-amine), DMA ($C_2$-amine), trimethylamine ($C_3$-amine), and butylamine ($C_4$-amine). The detection of other SA-B than SA-DMA clusters indicates that other candidate bases could also play a crucial role in the complex atmosphere for nucleation. For example, a recent study conducted in Beijing highlights the importance of TMA, which can increase nucleation rate from SA-DMA system by 50% – 100% (Cai et al., 2023b). In the Po Valley, the signal intensity of $SA_4$-$NH_3$ was significantly higher than that of the pure $SA_4$-amine clusters (~2 times) even though amines (e.g., DMA) were proven to be more efficient (~3 orders of magnitude) than $NH_3$ in clustering (Almeida et al., 2013). SA-$NH_3$-Amine clusters could be found along with SA-$NH_3$ clusters in $SA_5$-B and $SA_6$-B. Similar patterns of the high fractions of SA−$NH_3$ and SA-$NH_3$-Amine clusters were also reported in the CLOUD chamber studies under relatively low DMA and high $NH_3$ conditions (Schobesberger et al., 2013). Therefore, it can be concluded that a large amount of $NH_3$ also participates in NPF in the Po Valley region. Meanwhile, with a much lower amount, amines may also play a crucial role in the formation of small clusters (SA-B) due to their high stabilization efficiencies.

Moreover, some SA-$NH_3$-Org and I-containing ion clusters were also observed on NPF days, but to a much lower extent than clusters involving $NH_3$ or DMA. It has been shown in previous CLOUD chamber studies that the oxidation products of anthropogenic volatile organic compounds (AVOCs, e.g., naphthalene, trimethylbenzene and toluene) can largely promote the formation rate of particles (Xiao et al., 2021). The I-containing ions (mainly $IO_3^-$) likely originated from the Adriatic Sea during the daytime. Since no large iodine clusters were identified in the APi-TOF (e.g., $(HIO_3)_{0-1}(I_2O_5)_n \cdot IO_3^-$, (He et al., 2021)), iodine-induced new particle formation in the Po Valley may not be as important as the pristine marine environment (Sipila et al., 2016). During NPF without growth days, the formation mechanism was similar to the NPF days regarding the ion cluster measurement (Fig. S5).

The SA monomer in the Po Valley can be observed during the peak hours (10:00 − 14:00 LT) in both NPF and non-NPF days, but much lower SA dimer or trimers were found in the non-NPF days (Figs. 4b, and S6). In the nighttime, the SA concentrations were close to zero due to the scavenging of $SO_2$ and SA by the high RH (Fig. 1). During our sampling period, large amounts of organics were identified by the CI-APi-TOF. They were typically smaller than 400 Th with carbon numbers < 8 and oxygen numbers < 6 (Fig. S7). Due to the relatively high $NO_x$ levels (13 ppb) that can terminate the dimerization reactions (Yan et al., 2020), no OOM dimers were found, which is different from clean and biogenically dominated environments such as Hyytiälä (Lehtipalo et al., 2018). The compositions of OOMs were similar between NPF and non-NPF days but with different abundance. Extremely high abundances of nitrophenols and their homologous compounds were found on non-NPF days (~8 times higher than on

NPF days), likely caused by both of the enhanced primary (e.g., biomass burning (Mohr et al., 2013) and pesticide usage (Harrison et al., 2005)) and secondary (e.g., photochemical and/or aqueous-phase secondary formation) sources (Zheng et al., 2021; Gilardoni et al., 2016). $C_{2\text{-}4}H_{4,5}N_{0,1}O_{3,4}$ compounds were found to be 50% higher (Fig. S7) on non-NPF days likely caused by the enhanced heterogeneous reactions that form smaller organics such as carboxylic acids under higher RH conditions. Previous studies also reported aqueous-phase organic aerosol processing at high RH (Gilardoni et al., 2016) and high concentrations of carboxylic acids such as formic, oxalic, and malonic acids in the springtime in the Po Valley (Saarikoski et al., 2012). In general, the fraction of the abundance of nitrogen-containing OOMs (CHON) of total identified OOMs were 60% − 70%, which is close to the levels reported in polluted cities such as Nanjing (Nie et al., 2022) and Beijing (Guo et al., 2022). A slightly higher fraction of CHON compounds (73 %) was found during non-NPF days than NPF days (67 %), consistent with higher NOx and fine particulate matter levels (Fig. S8). It is likely associated with the stagnant meteorological conditions and accumulation of pollutants during the non-NPF days. However, the overall high amounts of CHON compounds and the lack of organic dimers make it unlikely that OOMs drive the NPF process (both clustering and initial growth, see e.g., Simon et al. (2020)). Their similar abundance on non-NPF and NPF days was also in line with the similar estimated GR for both types of days.

Throughout the entire sampling period, relatively high concentrations of fine particulate matters ($PM_{2.5}$) were measured, with a daily average of 17 μg $m^{-3}$ and a maximum value of 43 μg $m^{-3}$. Correspondingly, the hourly CS levels, which quantify the ability of pre-existing particles to scavenge gaseous precursors, ranged from $<1\times10^{-4}$ $s^{-1}$ to $3\times10^{-2}$ $s^{-1}$ with an average value of $5.4\times10^{-3}$ $s^{-1}$. Previous studies in polluted areas, such as Chinese megacities, have shown that NPF events are closely linked to CS levels (Cai et al., 2017). NPF probability was reported to decreased to 50% when CS was around $1\times10^{-2}$ $s^{-1}$ and completely shut off with CS of $6\times10^{-2}$ $s^{-1}$ (Du et al., 2022). However, in the Po Valley, we observed no strong influence of CS on NPF events, with only a slightly difference in CS during the noontime of non-NPF days (median: $9.4\times10^{-3}$ $s^{-1}$) than NPF days (median: $8.6\times10^{-3}$ $s^{-1}$).

### 3.4 Comparison between Po Valley and other environments

Even though the measured $J_{1.7}$ in Po Valley was at the same level of the values found in Chinese polluted megacities, it was much higher than in clean environments, such as the boreal forest of Hyytiälä in Finland, mountain sites of Jungfraujoch in Switzerland, and Chacaltaya in Bolivia (1.5 $cm^{-3}$ $s^{-1}$ – 2.0 $cm^{-3}$ $s^{-1}$, Fig. 5a). The average SA concentrations ($4.6\times10^{6}$ $cm^{-3}$, 10:00 – 14:00 LT) were comparable to the levels observed in polluted megacities in China (ranging from $3.9\times10^{6}$ $cm^{-3}$ to $7.4\times10^{6}$ $cm^{-3}$, Fig. 5c), but significantly higher than those in remote areas like Hyytiälä ($9\times10^{5}$ $cm^{-3}$) and the Jungfraujoch ($5\times10^{5}$ $cm^{-3}$). SA concentrations during NPF days ($8.6\times10^{6}$ $cm^{-3}$) in the Po Valley were twice as high as those on non-NPF days ($4\times10^{6}$ $cm^{-3}$). This difference may be linked to the significant variations (t-test, $p<0.05$) of $SO_2$ concentrations between NPF days (0.38 ppb) and non-NPF days (0.20 ppb). This contrasts with findings in Beijing, where similar or even higher levels of SA and $SO_2$ were observed during non-NPF days compared to NPF event days (Yan et al., 2021). The variations in $SO_2$ and SA concentrations in the Po Valley could possibly be attributed to differences of air masses, as indicated by higher RH on non-NPF days (53%) than on NPF days (38%) but similar temperature (NPF days: 288 K, non-NPF days: 287 K). On higher RH days, photochemistry may be suppressed, potentially reducing the formation of sulfuric acid and low volatile condensable vapors.

The overall CS in spring (median: $8.9\times10^{-3}$ $s^{-1}$) in the Po Valley was lower than that in other polluted cities ($1.5\times10^{-1}$ $s^{-1}$– $2.0\times10^{-1}$ $s^{-1}$), but significantly higher than that in clean environments ($2.0\times10^{-4}$ $s^{-1}$ (Hyytiälä and Jungfraujoch) – $3.0\times10^{-3}$ $s^{-1}$ (Chacaltaya with the influence of volcanoes), Fig. 5e). Contrary to Beijing or Shanghai where CS levels and efficiencies are the dominant factors for the NPF process (Du et al., 2022), NPF events in Po Valley are not strongly dependent on the CS levels, likely due to generally lower CS levels than the Asian megacities (Fig. S8). The strength of precursor sources

and their accumulation in the Po-Valley region might thus be more important for NPF to occur than the overall pre-existing sink for those precursors.

The average $PM_1$ concentrations during the sampling period was around 8 μg $m^{-3}$, significantly lower than New Delhi (268 μg $m^{-3}$), Beijing (33 μg $m^{-3}$, (Li et al., 2019)) and Shanghai (30 μg $m^{-3}$, (Song et al., 2023), Fig. S9). The major chemical compositions in $PM_1$ in Po Valley were similar to those in Beijing and Shanghai, with organics, ammonium nitrate, and ammonium sulfate being the most abundant components. However, $PM_1$ compositions in New Delhi differed from Po Valley and megacities in China. In New Delhi, strong biomass burning emissions with a high abundance of primary organics (155 μg $m^{-3}$, 58%) suppressed NPF events during the daytime from January to February but led to nocturnal particle growth, which is not observed in other polluted areas (Mishra et al., 2023).

Even with similar levels of CS and total $PM_1$ concentrations (NPF: 6.3 μg $m^{-3}$ and non-NPF: 6.5 μg $m^{-3}$) observed during noontime in Po Valley, the concentration of $NO_3^-$ increased by 50% on non-NPF days compared to NPF days, higher than the increase of $PM_1$ (3.1%) as shown in Fig. S9. A lower CS efficiency due to lower fraction of nitrate was reported to suppress the scavenge of NPF precursors in Beijing (Du et al., 2022), which may also have the similar influence in the Po Valley. The observed growth rate for 7 – 15 nm particles in the Po Valley was about 5.1 nm $h^{-1}$, comparable to other urban and remote sites (2.9 – 9.1 nm $h^{-1}$, Fig. 5f). The general similar growth rates among different types of environments were also reported in previous studies (Deng et al., 2020), which needs further investigation in future research.

For the basic gaseous precursors, the average concentration of $NH_3$ was ~10 ppb, which was in the same range as that found in the Chinese megacities (10 – 30 ppb) and much higher than those at remote sites (<0.1 ppb, Table S1). The high $NH_3$ can be attributed to agricultural activities such as fertilization, which were widely applied during springtime in the region. The strong interference of ammonia emitted from fertilization to NPF was also observed in Qvidja, an agricultural site in Southern Finland (Olin et al., 2022). During our sampling period, measured DMA were too close to the detection limit of the Vocus (Fig. S2), and lower than those observed in the Chinese megacities (10 – 40 ppt, Fig. 5d). In the spring season, DMA in the Po Valley cannot fully stabilize all atmospheric SA clusters and hence NPF is very sensitive to variations in the concentrations of the different stabilizers ($NH_3$, DMA, and as shown by our analysis likely only to a lower extent organics). This could explain the scattered correlation between the formation rate and SA concentrations on different days (Fig. 3).

Therefore, in the Po Valley region, the initial nucleation of frequent NPF is primarily attributed to high sulfuric acid concentrations and basic molecules, including ammonia and various amines. This mechanism is generally similar to what is observed in Chinese megacities. However, in the Po Valley region, DMA, a typical base in anthropogenic emission-influenced areas, is insufficient to stabilize the high levels of sulfuric acid, leading to the involvement of other basic molecules such as other type of amines and ammonia, likely originating from fertilization in the area. This involvement of ammonia and other amines differs from Chinese megacities such as Shanghai, where high levels of DMA were observed (~40 ppt, (Yao et al., 2018; Yao et al., 2016)). As insufficient DMA is available to stabilize all clusters, we speculate that the clustering is therefore sensitive to the abundance of amines. In that sense, during our sampling period, NPF in Po Valley seems to be more sensitive to the strength of certain emission sources of amines compared to megacity environments, where abundant DMA was observed. The abundant OOMs dominate the consecutive growth process, leading to a comparable GR to Chinese megacities such as Beijing and Shanghai. Due to the relatively lower CS than these megacities, the newly formed particles may however have a higher survival probability and provide more long-term surviving particles in the Po Valley, indicating a decisive role of NPF for Po-Valley aerosol and $PM_{2.5}$ concentrations.

## 4. Conclusions

In this study, we conducted a continuous two-month measurement campaign in the Italian Po Valley during springtime, where frequent NPF events were observed on 66% of all days. Through direct ion cluster measurement, kinetic models, and the comparison with the CLOUD chamber experiment, we have determined that sulfuric acid-base nucleation is the dominant formation mechanism in the Po Valley region. Abundant sulfuric acid and basic molecules, including amines and ammonia derived from agriculture activities, provided ample precursors for NPF events. In contrast to megacity environments, CS showed no significant difference between NPF event and non-event days, indicating that in Po Valley it is more the abundance of precursors than the variations in the sink controlling the occurrence of NPF. Furthermore, we observed that apart from DMA, a typical basic precursor, $NH_3$ and other amines were also likely to be involved in NPF in the Po Valley. This was supported by the high abundance of SA-$NH_3$ and SA-amine-$NH_3$ clusters measured by the APi-TOF during NPF events. DMA, while more efficient than ammonia, was insufficient to stabilize all SA during our sampling period. This resulted in a more scattered correlation between sulfuric acid concentrations and measured formation rates compared to Chinese megacities. In that sense, we could show that the clustering during NPF is clearly distinct between polluted megacity environments and polluted semi-urbanized regions such as Po Valley. Similar to Beijing, we found that OOMs did not play a decisive role in the initial cluster formations, likely due to the absence of ultra-low volatility organics (typical OOM dimers) in the ions and neutral cluster measurements. However, low-volatility organics were abundant enough to induce fast growth processes above 3 nm. The comparable GR and formation rates, along with lower efficient CS compared to megacity environments, indicate a high survival probability for the newly formed particles. Therefore, NPF is likely to play an important role in the fine particle concentrations and pollution levels in the Po Valley region. Further reductions of key NPF species, including $SO_2$, amines and $NH_3$, can contribute to suppressing NPF event frequency and lowering particle numbers. This, in turn, would improve air quality in the Po Valley region.

## Data availability

Data are available from the authors upon request.

## Competing interests

At least one of the (co-)authors is a member of the editorial board of Atmospheric Chemistry and Physics

## Author contributions

JC, DS, FB, and MK designed the research. JC, JS, YFG, SH, MP, AN, FM, SD, MR, NZ and CM collected the data at the SPC site. JC, JS, YG, ST, RY, DA, QZ, DS and FB interpreted the data. MP, WH, YL, GC, LQ, KL, YG, CW, WN, JK, CM, QZ, DS, FB helped to improve the manuscript. JC, JS, DS, and FB wrote the manuscript with contributions from all co-authors. All authors have given approval to the final version of this manuscript.

## Acknowledgements

The work is supported by the Academy of Finland (Center of Excellence in Atmospheric Sciences, project no. 307331, PROFI3 funding no. 311932, and ACCC Flagship no. 337549), the European Research Council via ATM-GTP (no. 742206), Consolidator grant INTEGRATE (no. 865799) and CHAPAs (no. 850614), the European Union's Horizon 2020 research and innovation programme (project FORCeS under grant agreement no. 821205, H2020-INFRAIA-2020-1 grant agreement no. 101008004, Marie Skłodowska–Curie grant agreement no. 895875 (NPF-PANDA), the Vienna Science and Technology Fund (WWTF) through project VRG22-003, Jenny and Antti Wihuri Foundation, and the Knut and Alice Wallenberg Foundation (WAF project CLOUDFORM, grant no. 2017.0165). The authors also would like to thank the effort from all the researchers in the SPC site. The authors would

558 also like to thank Chenjuan Deng, Mao Xiao and Lubna Dada for providing the supporting data from
559 Beijing and CLOUD chamber experiment.

560

## Reference


Almeida, J., Schobesberger, S., Kurten, A., Ortega, I. K., Kupiainen-Maatta, O., Praplan, A. P., Adamov, A., Amorim, A., Bianchi, F., Breitenlechner, M., David, A., Dommen, J., Donahue, N. M., Downard, A., Dunne, E., Duplissy, J., Ehrhart, S., Flagan, R. C., Franchin, A., Guida, R., Hakala, J., Hansel, A., Heinritzi, M., Henschel, H., Jokinen, T., Junninen, H., Kajos, M., Kangasluoma, J., Keskinen, H., Kupc, A., Kurten, T., Kvashin, A. N., Laaksonen, A., Lehtipalo, K., Leiminger, M., Leppa, J., Loukonen, V., Makhmutov, V., Mathot, S., McGrath, M. J., Nieminen, T., Olenius, T., Onnela, A., Petaja, T., Riccobono, F., Riipinen, I., Rissanen, M., Rondo, L., Ruuskanen, T., Santos, F. D., Sarnela, N., Schallhart, S., Schnitzhofer, R., Seinfeld, J. H., Simon, M., Sipila, M., Stozhkov, Y., Stratmann, F., Tome, A., Trostl, J., Tsagkogeorgas, G., Vaattovaara, P., Viisanen, Y., Virtanen, A., Vrtala, A., Wagner, P. E., Weingartner, E., Wex, H., Williamson, C., Wimmer, D., Ye, P., Yli-Juuti, T., Carslaw, K. S., Kulmala, M., Curtius, J., Baltensperger, U., Worsnop, D. R., Vehkamaki, H., and Kirkby, J.: Molecular understanding of sulphuric acid-amine particle nucleation in the atmosphere, Nature, 502, 359-363, 10.1038/nature12663, 2013.

Boulon, J., Sellegri, K., Venzac, H., Picard, D., Weingartner, E., Wehrle, G., Collaud Coen, M., Bütikofer, R., Flückiger, E., Baltensperger, U., and Laj, P.: New particle formation and ultrafine charged aerosol climatology at a high altitude site in the Alps (Jungfraujoch, 3580 m a.s.l., Switzerland), Atmospheric Chemistry and Physics, 10, 9333-9349, 10.5194/acp-10-9333-2010, 2010.

Brean, J., Beddows, D. C. S., Shi, Z., Temime-Roussel, B., Marchand, N., Querol, X., Alastuey, A., Minguillón, M. C., and Harrison, R. M.: Molecular insights into new particle formation in Barcelona, Spain, Atmospheric Chemistry and Physics, 20, 10029-10045, 10.5194/acp-20-10029-2020, 2020.

Cai, J., Daellenbach, K. R., Wu, C., Zheng, Y., Zheng, F., Du, W., Haslett, S. L., Chen, Q., Kulmala, M., and Mohr, C.: Characterization of offline analysis of particulate matter with FIGAERO-CIMS, Atmospheric Measurement Techniques, 16, 1147-1165, 10.5194/amt-16-1147-2023, 2023a.

Cai, J., Wu, C., Wang, J., Du, W., Zheng, F., Hakala, S., Fan, X., Chu, B., Yao, L., Feng, Z., Liu, Y., Sun, Y., Zheng, J., Yan, C., Bianchi, F., Kulmala, M., Mohr, C., and Daellenbach, K. R.: Influence of organic aerosol molecular composition on particle absorptive properties in autumn Beijing, Atmospheric Chemistry and Physics, 22, 1251-1269, 10.5194/acp-22-1251-2022, 2022.

Cai, R., Attoui, M., Jiang, J., Korhonen, F., Hao, J., Petäjä, T., and Kangasluoma, J.: Characterization of a high-resolution supercritical differential mobility analyzer at reduced flow rates, Aerosol Science and Technology, 52, 1332-1343, 10.1080/02786826.2018.1520964, 2018.

Cai, R., Yang, D., Fu, Y., Wang, X., Li, X., Ma, Y., Hao, J., Zheng, J., and Jiang, J.: Aerosol surface area concentration: a governing factor in new particle formation in Beijing, Atmospheric Chemistry and Physics, 17, 12327-12340, 10.5194/acp-17-12327-2017, 2017.

Cai, R., Yin, R., Li, X., Xie, H.-B., Yang, D., Kerminen, V.-M., Smith, J. N., Ma, Y., Hao, J., Chen, J., Kulmala, M., Zheng, J., Jiang, J., and Elm, J.: Significant contributions of trimethylamine to sulfuric acid nucleation in polluted environments, npj Climate and Atmospheric Science, 6, 10.1038/s41612-023-00405-3, 2023b.

Cai, R., Yan, C., Yang, D., Yin, R., Lu, Y., Deng, C., Fu, Y., Ruan, J., Li, X., Kontkanen, J., Zhang, Q., Kangasluoma, J., Ma, Y., Hao, J., Worsnop, D. R., Bianchi, F., Paasonen, P., Kerminen, V. M., Liu, Y., Wang, L., Zheng, J., Kulmala, M., and Jiang, J.: Sulfuric acid–amine nucleation in urban Beijing, Atmos. Chem. Phys., 21, 2457-2468, 10.5194/acp-21-2457-2021, 2021.

Chu, B., Kerminen, V.-M., Bianchi, F., Yan, C., Petäjä, T., and Kulmala, M.: Atmospheric new particle formation in China, Atmospheric Chemistry and Physics, 19, 115-138, 10.5194/acp-19-115-2019, 2019.

Dada, L., Chellapermal, R., Buenrostro Mazon, S., Paasonen, P., Lampilahti, J., Manninen, H. E., Junninen, H., Petäjä, T., Kerminen, V.-M., and Kulmala, M.: Refined classification and characterization of atmospheric new-particle formation events using air ions, Atmospheric Chemistry and Physics, 18, 17883-17893, 10.5194/acp-18-17883-2018, 2018.

Dai, L., Wang, H., Zhou, L., An, J., Tang, L., Lu, C., Yan, W., Liu, R., Kong, S., Chen, M., Lee, S., and Yu, H.: Regional and local new particle formation events observed in the Yangtze River Delta region, China, Journal of Geophysical Research: Atmospheres, 122, 2389-2402, 10.1002/2016jd026030, 2017.

Dal Maso, M., Kulmala, M., Riipinen, I., Wagner, R., Hussein, T., Aalto, P. P., and Lehtinen, K. E. J.: Formation and growth of fresh atmospheric aerosols: eight years of aerosol size distribution data from SMEAR II, Hyytiala, Finland, Boreal Environment Research, 10, 323-336, 2005.
de Jesus, A. L., Rahman, M. M., Mazaheri, M., Thompson, H., Knibbs, L. D., Jeong, C., Evans, G., Nei, W., Ding, A., Qiao, L., Li, L., Portin, H., Niemi, J. V., Timonen, H., Luoma, K., Petaja, T., Kulmala, M., Kowalski, M., Peters, A., Cyrys, J., Ferrero, L., Manigrasso, M., Avino, P., Buonano, G., Reche, C., Querol, X., Beddows, D., Harrison, R. M., Sowlat, M. H., Sioutas, C., and Morawska, L.: Ultrafine particles and PM(2.5) in the air of cities around the world: Are they representative of each other?, Environ Int, 129, 118-135, 10.1016/j.envint.2019.05.021, 2019.
Decesari, S., Allan, J., Plass-Duelmer, C., Williams, B. J., Paglione, M., Facchini, M. C., O'Dowd, C., Harrison, R. M., Gietl, J. K., Coe, H., Giulianelli, L., Gobbi, G. P., Lanconelli, C., Carbone, C., Worsnop, D., Lambe, A. T., Ahern, A. T., Moretti, F., Tagliavini, E., Elste, T., Gilge, S., Zhang, Y., and Dall'Osto, M.: Measurements of the aerosol chemical composition and mixing state in the Po Valley using multiple spectroscopic techniques, Atmospheric Chemistry and Physics, 14, 12109-12132, 10.5194/acp-14-12109-2014, 2014.
Deng, C., Fu, Y., Dada, L., Yan, C., Cai, R., Yang, D., Zhou, Y., Yin, R., Lu, Y., Li, X., Qiao, X., Fan, X., Nie, W., Kontkanen, J., Kangasluoma, J., Chu, B., Ding, A., Kerminen, V. M., Paasonen, P., Worsnop, D. R., Bianchi, F., Liu, Y., Zheng, J., Wang, L., Kulmala, M., and Jiang, J.: Seasonal Characteristics of New Particle Formation and Growth in Urban Beijing, Environ Sci Technol, 54, 8547-8557, 10.1021/acs.est.0c00808, 2020.
Du, W., Cai, J., Zheng, F., Yan, C., Zhou, Y., Guo, Y., Chu, B., Yao, L., Heikkinen, L. M., Fan, X., Wang, Y., Cai, R., Hakala, S., Chan, T., Kontkanen, J., Tuovinen, S., Petäjä, T., Kangasluoma, J., Bianchi, F., Paasonen, P., Sun, Y., Kerminen, V.-M., Liu, Y., Daellenbach, K. R., Dada, L., and Kulmala, M.: Influence of Aerosol Chemical Composition on Condensation Sink Efficiency and New Particle Formation in Beijing, Environmental Science & Technology Letters, 9, 375-382, 10.1021/acs.estlett.2c00159, 2022.
Fan, X., Cai, J., Yan, C., Zhao, J., Guo, Y., Li, C., Dällenbach, K. R., Zheng, F., Lin, Z., Chu, B., Wang, Y., Dada, L., Zha, Q., Du, W., Kontkanen, J., Kurtén, T., Iyer, S., Kujansuu, J. T., Petäjä, T., Worsnop, D. R., Kerminen, V.-M., Liu, Y., Bianchi, F., Tham, Y. J., Yao, L., and Kulmala, M.: Atmospheric gaseous hydrochloric and hydrobromic acid in urban Beijing, China: detection, source identification and potential atmospheric impacts, Atmospheric Chemistry and Physics, 21, 11437-11452, 10.5194/acp-21-11437-2021, 2021.
Fernández de la Mora, J. and Kozlowski, J.: Hand-held differential mobility analyzers of high resolution for 1–30nm particles: Design and fabrication considerations, Journal of Aerosol Science, 57, 45-53, 10.1016/j.jaerosci.2012.10.009, 2013.
Fu, Y., Xue, M., Cai, R., Kangasluoma, J., and Jiang, J.: Theoretical and experimental analysis of the core sampling method: Reducing diffusional losses in aerosol sampling line, Aerosol Science and Technology, 53, 793-801, 10.1080/02786826.2019.1608354, 2019.
Gilardoni, S., Massoli, P., Paglione, M., Giulianelli, L., Carbone, C., Rinaldi, M., Decesari, S., Sandrini, S., Costabile, F., Gobbi, G. P., Pietrogrande, M. C., Visentin, M., Scotto, F., Fuzzi, S., and Facchini, M. C.: Direct observation of aqueous secondary organic aerosol from biomass-burning emissions, Proc Natl Acad Sci U S A, 113, 10013-10018, 10.1073/pnas.1602212113, 2016.
Guo, S., Hu, M., Zamora, M. L., Peng, J., Shang, D., Zheng, J., Du, Z., Wu, Z., Shao, M., Zeng, L., Molina, M. J., and Zhang, R.: Elucidating severe urban haze formation in China, Proc Natl Acad Sci U S A, 111, 17373-17378, 10.1073/pnas.1419604111, 2014.
Guo, S., Hu, M., Peng, J., Wu, Z., Zamora, M. L., Shang, D., Du, Z., Zheng, J., Fang, X., Tang, R., Wu, Y., Zeng, L., Shuai, S., Zhang, W., Wang, Y., Ji, Y., Li, Y., Zhang, A. L., Wang, W., Zhang, F., Zhao, J., Gong, X., Wang, C., Molina, M. J., and Zhang, R.: Remarkable nucleation and growth of ultrafine particles from vehicular exhaust, Proceedings of the National Academy of Sciences, 10.1073/pnas.1916366117, 2020.
Guo, Y., Yan, C., Liu, Y., Qiao, X., Zheng, F., Zhang, Y., Zhou, Y., Li, C., Fan, X., Lin, Z., Feng, Z., Zhang, Y., Zheng, P., Tian, L., Nie, W., Wang, Z., Huang, D., Daellenbach, K. R., Yao, L., Dada, L., Bianchi, F., Jiang,

J., Liu, Y., Kerminen, V.-M., and Kulmala, M.: Seasonal variation in oxygenated organic molecules in urban Beijing and their contribution to secondary organic aerosol, Atmospheric Chemistry and Physics, 22, 10077-10097, 10.5194/acp-22-10077-2022, 2022.
Hamed, A., Joutsensaari, J., Mikkonen, S., Sogacheva, L., Dal Maso, M., Kulmala, M., Cavalli, F., Fuzzi, S., Facchini, M. C., Decesari, S., Mircea, M., Lehtinen, K. E. J., and Laaksonen, A.: Nucleation and growth of new particles in Po Valley, Italy, Atmos. Chem. Phys., 7, 355-376, 10.5194/acp-7-355-2007, 2007.
Harrison, M. A. J., Barra, S., Borghesi, D., Vione, D., Arsene, C., and Iulian Olariu, R.: Nitrated phenols in the atmosphere: a review, Atmospheric Environment, 39, 231-248, 10.1016/j.atmosenv.2004.09.044, 2005.
He, X. C., Tham, Y. J., Dada, L., Wang, M., Finkenzeller, H., Stolzenburg, D., Iyer, S., Simon, M., Kurten, A., Shen, J., Rorup, B., Rissanen, M., Schobesberger, S., Baalbaki, R., Wang, D. S., Koenig, T. K., Jokinen, T., Sarnela, N., Beck, L. J., Almeida, J., Amanatidis, S., Amorim, A., Ataei, F., Baccarini, A., Bertozzi, B., Bianchi, F., Brilke, S., Caudillo, L., Chen, D., Chiu, R., Chu, B., Dias, A., Ding, A., Dommen, J., Duplissy, J., El Haddad, I., Gonzalez Carracedo, L., Granzin, M., Hansel, A., Heinritzi, M., Hofbauer, V., Junninen, H., Kangasluoma, J., Kemppainen, D., Kim, C., Kong, W., Krechmer, J. E., Kvashin, A., Laitinen, T., Lamkaddam, H., Lee, C. P., Lehtipalo, K., Leiminger, M., Li, Z., Makhmutov, V., Manninen, H. E., Marie, G., Marten, R., Mathot, S., Mauldin, R. L., Mentler, B., Mohler, O., Muller, T., Nie, W., Onnela, A., Petaja, T., Pfeifer, J., Philippov, M., Ranjithkumar, A., Saiz-Lopez, A., Salma, I., Scholz, W., Schuchmann, S., Schulze, B., Steiner, G., Stozhkov, Y., Tauber, C., Tome, A., Thakur, R. C., Vaisanen, O., Vazquez-Pufleau, M., Wagner, A. C., Wang, Y., Weber, S. K., Winkler, P. M., Wu, Y., Xiao, M., Yan, C., Ye, Q., Ylisirnio, A., Zauner-Wieczorek, M., Zha, Q., Zhou, P., Flagan, R. C., Curtius, J., Baltensperger, U., Kulmala, M., Kerminen, V. M., Kurten, T., Donahue, N. M., Volkamer, R., Kirkby, J., Worsnop, D. R., and Sipila, M.: Role of iodine oxoacids in atmospheric aerosol nucleation, Science, 371, 589-595, 10.1126/science.abe0298, 2021.
Hemmilä, M., Hellén, H., Virkkula, A., Makkonen, U., Praplan, A. P., Kontkanen, J., Ahonen, L., Kulmala, M., and Hakola, H.: Amines in boreal forest air at SMEAR II station in Finland, Atmospheric Chemistry and Physics, 18, 6367-6380, 10.5194/acp-18-6367-2018, 2018.
Jokinen, T., Sipilä, M., Junninen, H., Ehn, M., Lönn, G., Hakala, J., Petäjä, T., Mauldin, R. L., Kulmala, M., and Worsnop, D. R.: Atmospheric sulphuric acid and neutral cluster measurements using CI-APi-TOF, Atmospheric Chemistry and Physics, 12, 4117-4125, 10.5194/acp-12-4117-2012, 2012.
Junninen, H., Ehn, M., Petäjä, T., Luosujärvi, L., Kotiaho, T., Kostiainen, R., Rohner, U., Gonin, M., Fuhrer, K., Kulmala, M., and Worsnop, D. R.: A high-resolution mass spectrometer to measure atmospheric ion composition, Atmospheric Measurement Techniques, 3, 1039-1053, 10.5194/amt-3-1039-2010, 2010.
Kangasluoma, J., Ahonen, L. R., Laurila, T. M., Cai, R., Enroth, J., Mazon, S. B., Korhonen, F., Aalto, P. P., Kulmala, M., Attoui, M., and Petäjä, T.: Laboratory verification of a new high flow differential mobility particle sizer, and field measurements in Hyytiälä, Journal of Aerosol Science, 124, 1-9, 10.1016/j.jaerosci.2018.06.009, 2018.
Kangasluoma, J., Attoui, M., Junninen, H., Lehtipalo, K., Samodurov, A., Korhonen, F., Sarnela, N., Schmidt-Ott, A., Worsnop, D., Kulmala, M., and Petäjä, T.: Sizing of neutral sub 3nm tungsten oxide clusters using Airmodus Particle Size Magnifier, Journal of Aerosol Science, 87, 53-62, 10.1016/j.jaerosci.2015.05.007, 2015.
Kangasluoma, J., Franchin, A., Duplissy, J., Ahonen, L., Korhonen, F., Attoui, M., Mikkilä, J., Lehtipalo, K., Vanhanen, J., Kulmala, M., and Petäjä, T.: Operation of the Airmodus A11 nano Condensation Nucleus Counter at various inlet pressures and various operation temperatures, and design of a new inlet system, Atmospheric Measurement Techniques, 9, 2977-2988, 10.5194/amt-9-2977-2016, 2016.
Kirkby, J., Curtius, J., Almeida, J., Dunne, E., Duplissy, J., Ehrhart, S., Franchin, A., Gagne, S., Ickes, L., Kurten, A., Kupc, A., Metzger, A., Riccobono, F., Rondo, L., Schobesberger, S., Tsagkogeorgas, G., Wimmer, D., Amorim, A., Bianchi, F., Breitenlechner, M., David, A., Dommen, J., Downard, A., Ehn, M., Flagan, R. C., Haider, S., Hansel, A., Hauser, D., Jud, W., Junninen, H., Kreissl, F., Kvashin, A., Laaksonen, A., Lehtipalo, K., Lima, J., Lovejoy, E. R., Makhmutov, V., Mathot, S., Mikkila, J., Minginette, P., Mogo,

S., Nieminen, T., Onnela, A., Pereira, P., Petaja, T., Schnitzhofer, R., Seinfeld, J. H., Sipila, M., Stozhkov, Y., Stratmann, F., Tome, A., Vanhanen, J., Viisanen, Y., Vrtala, A., Wagner, P. E., Walther, H., Weingartner, E., Wex, H., Winkler, P. M., Carslaw, K. S., Worsnop, D. R., Baltensperger, U., and Kulmala, M.: Role of sulphuric acid, ammonia and galactic cosmic rays in atmospheric aerosol nucleation, Nature, 476, 429-433, 10.1038/nature10343, 2011.

Kirkby, J., Duplissy, J., Sengupta, K., Frege, C., Gordon, H., Williamson, C., Heinritzi, M., Simon, M., Yan, C., Almeida, J., Trostl, J., Nieminen, T., Ortega, I. K., Wagner, R., Adamov, A., Amorim, A., Bernhammer, A. K., Bianchi, F., Breitenlechner, M., Brilke, S., Chen, X., Craven, J., Dias, A., Ehrhart, S., Flagan, R. C., Franchin, A., Fuchs, C., Guida, R., Hakala, J., Hoyle, C. R., Jokinen, T., Junninen, H., Kangasluoma, J., Kim, J., Krapf, M., Kurten, A., Laaksonen, A., Lehtipalo, K., Makhmutov, V., Mathot, S., Molteni, U., Onnela, A., Perakyla, O., Piel, F., Petaja, T., Praplan, A. P., Pringle, K., Rap, A., Richards, N. A., Riipinen, I., Rissanen, M. P., Rondo, L., Sarnela, N., Schobesberger, S., Scott, C. E., Seinfeld, J. H., Sipila, M., Steiner, G., Stozhkov, Y., Stratmann, F., Tome, A., Virtanen, A., Vogel, A. L., Wagner, A. C., Wagner, P. E., Weingartner, E., Wimmer, D., Winkler, P. M., Ye, P., Zhang, X., Hansel, A., Dommen, J., Donahue, N. M., Worsnop, D. R., Baltensperger, U., Kulmala, M., Carslaw, K. S., and Curtius, J.: Ion-induced nucleation of pure biogenic particles, Nature, 533, 521-526, 10.1038/nature17953, 2016.

Kontkanen, J., Järvinen, E., Manninen, H. E., Lehtipalo, K., Kangasluoma, J., Decesari, S., Gobbi, G. P., Laaksonen, A., Petäjä, T., and Kulmala, M.: High concentrations of sub-3nm clusters and frequent new particle formation observed in the Po Valley, Italy, during the PEGASOS 2012 campaign, Atmospheric Chemistry and Physics, 16, 1919-1935, 10.5194/acp-16-1919-2016, 2016.

Kontkanen, J., Lehtipalo, K., Ahonen, L., Kangasluoma, J., Manninen, H. E., Hakala, J., Rose, C., Sellegri, K., Xiao, S., Wang, L., Qi, X., Nie, W., Ding, A., Yu, H., Lee, S., Kerminen, V.-M., Petäjä, T., and Kulmala, M.: Measurements of sub-3 nm particles using a particle size magnifier in different environments: from clean mountain top to polluted megacities, Atmospheric Chemistry and Physics, 17, 2163-2187, 10.5194/acp-17-2163-2017, 2017.

Kulmala, M., Kerminen, V. M., Petäjä, T., Ding, A. J., and Wang, L.: Atmospheric gas-to-particle conversion: why NPF events are observed in megacities?, Faraday Discussions, 200, 271-288, 10.1039/C6FD00257A, 2017.

Kulmala, M., Petäjä, T., Nieminen, T., Sipilä, M., Manninen, H. E., Lehtipalo, K., Dal Maso, M., Aalto, P. P., Junninen, H., Paasonen, P., Riipinen, I., Lehtinen, K. E. J., Laaksonen, A., and Kerminen, V.-M.: Measurement of the nucleation of atmospheric aerosol particles, Nature Protocols, 7, 1651-1667, 10.1038/nprot.2012.091, 2012.

Kulmala, M., Junninen, H., Dada, L., Salma, I., Weidinger, T., Thén, W., Vörösmarty, M., Komsaare, K., Stolzenburg, D., Cai, R., Yan, C., Li, X., Deng, C., Jiang, J., Petäjä, T., Nieminen, T., and Kerminen, V.-M.: Quiet New Particle Formation in the Atmosphere, Frontiers in Environmental Science, 10, 10.3389/fenvs.2022.912385, 2022.

Kulmala, M., Kontkanen, J., Junninen, H., Lehtipalo, K., Manninen, H. E., Nieminen, T., Petäjä, T., Sipilä, M., Schobesberger, S., Rantala, P., Franchin, A., Jokinen, T., Järvinen, E., Äijälä, M., Kangasluoma, J., Hakala, J., Aalto, P. P., Paasonen, P., Mikkilä, J., Vanhanen, J., Aalto, J., Hakola, H., Makkonen, U., Ruuskanen, T., Mauldin, R. L., Duplissy, J., Vehkamäki, H., Bäck, J., Kortelainen, A., Riipinen, I., Kurtén, T., Johnston, M. V., Smith, J. N., Ehn, M., Mentel, T. F., Lehtinen, K. E. J., Laaksonen, A., Kerminen, V.-M., and Worsnop, D. R.: Direct Observations of Atmospheric Aerosol Nucleation, Science, 339, 943-946, 10.1126/science.1227385, 2013.

Kulmala, M., Dada, L., Daellenbach, K. R., Yan, C., Stolzenburg, D., Kontkanen, J., Ezhova, E., Hakala, S., Tuovinen, S., Kokkonen, T. V., Kurppa, M., Cai, R., Zhou, Y., Yin, R., Baalbaki, R., Chan, T., Chu, B., Deng, C., Fu, Y., Ge, M., He, H., Heikkinen, L., Junninen, H., Liu, Y., Lu, Y., Nie, W., Rusanen, A., Vakkari, V., Wang, Y., Yang, G., Yao, L., Zheng, J., Kujansuu, J., Kangasluoma, J., Petaja, T., Paasonen, P., Jarvi, L., Worsnop, D., Ding, A., Liu, Y., Wang, L., Jiang, J., Bianchi, F., and Kerminen, V. M.: Is reducing new particle formation a plausible solution to mitigate particulate air pollution in Beijing and other Chinese megacities?, Faraday Discuss, 226, 334-347, 10.1039/d0fd00078g, 2021.

763 Kurten, A., Rondo, L., Ehrhart, S., and Curtius, J.: Calibration of a chemical ionization mass
764 spectrometer for the measurement of gaseous sulfuric acid, J Phys Chem A, 116, 6375-6386,
765 10.1021/jp212123n, 2012.
766 Lampimäki, M., Baalbaki, R., Ahonen, L., Korhonen, F., Cai, R., Chan, T., Stolzenburg, D., Petäjä, T.,
767 Kangasluoma, J., Vanhanen, J., and Lehtipalo, K.: Novel aerosol diluter – Size dependent
768 characterization down to 1 nm particle size, Journal of Aerosol Science, 172, 106180,
769 https://doi.org/10.1016/j.jaerosci.2023.106180, 2023.
770 Lehtipalo, K., Ahonen, L. R., Baalbaki, R., Sulo, J., Chan, T., Laurila, T., Dada, L., Duplissy, J., Miettinen,
771 E., Vanhanen, J., Kangasluoma, J., Kulmala, M., Petäjä, T., and Jokinen, T.: The standard operating
772 procedure for Airmodus Particle Size Magnifier and nano-Condensation Nucleus Counter, Journal of
773 Aerosol Science, 159, 10.1016/j.jaerosci.2021.105896, 2022.
774 Lehtipalo, K., Yan, C., Dada, L., Bianchi, F., Xiao, M., Wagner, R., Stolzenburg, D., Ahonen, L. R., Amorim,
775 A., Baccarini, A., Bauer, P. S., Baumgartner, B., Bergen, A., Bernhammer, A.-K., Breitenlechner, M.,
776 Brilke, S., Buchholz, A., Mazon, S. B., Chen, D., Chen, X., Dias, A., Dommen, J., Draper, D. C., Duplissy,
777 J., Ehn, M., Finkenzeller, H., Fischer, L., Frege, C., Fuchs, C., Garmash, O., Gordon, H., Hakala, J., He, X.,
778 Heikkinen, L., Heinritzi, M., Helm, J. C., Hofbauer, V., Hoyle, C. R., Jokinen, T., Kangasluoma, J.,
779 Kerminen, V.-M., Kim, C., Kirkby, J., Kontkanen, J., Kürten, A., Lawler, M. J., Mai, H., Mathot, S., Mauldin,
780 R. L., Molteni, U., Nichman, L., Nie, W., Nieminen, T., Ojdanic, A., Onnela, A., Passananti, M., Petäjä,
781 T., Piel, F., Pospisilova, V., Quéléver, L. L. J., Rissanen, M. P., Rose, C., Sarnela, N., Schallhart, S.,
782 Schuchmann, S., Sengupta, K., Simon, M., Sipilä, M., Tauber, C., Tomé, A., Tröstl, J., Väisänen, O., Vogel,
783 A. L., Volkamer, R., Wagner, A. C., Wang, M., Weitz, L., Wimmer, D., Ye, P., Ylisirniö, A., Zha, Q., Carslaw,
784 K. S., Curtius, J., Donahue, N. M., Flagan, R. C., Hansel, A., Riipinen, I., Virtanen, A., Winkler, P. M.,
785 Baltensperger, U., Kulmala, M., and Worsnop, D. R.: Multicomponent new particle formation from
786 sulfuric acid, ammonia, and biogenic vapors, Science Advances, 4, eaau5363,
787 doi:10.1126/sciadv.aau5363, 2018.
788 Li, H., Cheng, J., Zhang, Q., Zheng, B., Zhang, Y., Zheng, G., and He, K.: Rapid transition in winter aerosol
789 composition in Beijing from 2014 to 2017: response to clean air actions, Atmospheric Chemistry and
790 Physics, 19, 11485-11499, 10.5194/acp-19-11485-2019, 2019.
791 Liu, S., Hu, M., Wu, Z., Wehner, B., Wiedensohler, A., and Cheng, Y.: Aerosol number size distribution
792 and new particle formation at a rural/coastal site in Pearl River Delta (PRD) of China, Atmospheric
793 Environment, 42, 6275-6283, 10.1016/j.atmosenv.2008.01.063, 2008.
794 Manninen, H. E., Nieminen, T., Asmi, E., Gagné, S., Häkkinen, S., Lehtipalo, K., Aalto, P., Vana, M.,
795 Mirme, A., Mirme, S., Hõrrak, U., Plass-Dülmer, C., Stange, G., Kiss, G., Hoffer, A., Törő, N., Moerman,
796 M., Henzing, B., de Leeuw, G., Brinkenberg, M., Kouvarakis, G. N., Bougiatioti, A., Mihalopoulos, N.,
797 O'Dowd, C., Ceburnis, D., Arneth, A., Svenningsson, B., Swietlicki, E., Tarozzi, L., Decesari, S., Facchini,
798 M. C., Birmili, W., Sonntag, A., Wiedensohler, A., Boulon, J., Sellegri, K., Laj, P., Gysel, M., Bukowiecki,
799 N., Weingartner, E., Wehrle, G., Laaksonen, A., Hamed, A., Joutsensaari, J., Petäjä, T., Kerminen, V. M.,
800 and Kulmala, M.: EUCAARI ion spectrometer measurements at 12 European sites – analysis of new
801 particle formation events, Atmos. Chem. Phys., 10, 7907-7927, 10.5194/acp-10-7907-2010, 2010.
802 Mishra, S., Tripathi, S. N., Kanawade, V. P., Haslett, S. L., Dada, L., Ciarelli, G., Kumar, V., Singh, A.,
803 Bhattu, D., Rastogi, N., Daellenbach, K. R., Ganguly, D., Gargava, P., Slowik, J. G., Kulmala, M., Mohr,
804 C., El-Haddad, I., and Prevot, A. S. H.: Rapid night-time nanoparticle growth in Delhi driven by biomass-
805 burning emissions, Nature Geoscience, 16, 224-230, 10.1038/s41561-023-01138-x, 2023.
806 Mohr, C., Lopez-Hilfiker, F. D., Zotter, P., Prevot, A. S., Xu, L., Ng, N. L., Herndon, S. C., Williams, L. R.,
807 Franklin, J. P., Zahniser, M. S., Worsnop, D. R., Knighton, W. B., Aiken, A. C., Gorkowski, K. J., Dubey,
808 M. K., Allan, J. D., and Thornton, J. A.: Contribution of nitrated phenols to wood burning brown carbon
809 light absorption in Detling, United Kingdom during winter time, Environ Sci Technol, 47, 6316-6324,
810 10.1021/es400683v, 2013.
811 Nie, W., Yan, C., Huang, D. D., Wang, Z., Liu, Y., Qiao, X., Guo, Y., Tian, L., Zheng, P., Xu, Z., Li, Y., Xu, Z.,
812 Qi, X., Sun, P., Wang, J., Zheng, F., Li, X., Yin, R., Dallenbach, K. R., Bianchi, F., Petäjä, T., Zhang, Y.,
813 Wang, M., Schervish, M., Wang, S., Qiao, L., Wang, Q., Zhou, M., Wang, H., Yu, C., Yao, D., Guo, H., Ye,

P., Lee, S., Li, Y. J., Liu, Y., Chi, X., Kerminen, V.-M., Ehn, M., Donahue, N. M., Wang, T., Huang, C., Kulmala, M., Worsnop, D., Jiang, J., and Ding, A.: Secondary organic aerosol formed by condensing anthropogenic vapours over China's megacities, Nature Geoscience, 15, 255-261, 10.1038/s41561-022-00922-5, 2022.

Paasonen, P., Nieminen, T., Asmi, E., Manninen, H. E., Petäjä, T., Plass-Dülmer, C., Flentje, H., Birmili, W., Wiedensohler, A., Hõrrak, U., Metzger, A., Hamed, A., Laaksonen, A., Facchini, M. C., Kerminen, V. M., and Kulmala, M.: On the roles of sulphuric acid and low-volatility organic vapours in the initial steps of atmospheric new particle formation, Atmospheric Chemistry and Physics, 10, 11223-11242, 10.5194/acp-10-11223-2010, 2010.

Paglione, M., Decesari, S., Rinaldi, M., Tarozzi, L., Manarini, F., Gilardoni, S., Facchini, M. C., Fuzzi, S., Bacco, D., Trentini, A., Pandis, S. N., and Nenes, A.: Historical Changes in Seasonal Aerosol Acidity in the Po Valley (Italy) as Inferred from Fog Water and Aerosol Measurements, Environ Sci Technol, 55, 7307-7315, 10.1021/acs.est.1c00651, 2021.

Paglione, M., Saarikoski, S., Carbone, S., Hillamo, R., Facchini, M. C., Finessi, E., Giulianelli, L., Carbone, C., Fuzzi, S., Moretti, F., Tagliavini, E., Swietlicki, E., Eriksson Stenström, K., Prévôt, A. S. H., Massoli, P., Canaragatna, M., Worsnop, D., and Decesari, S.: Primary and secondary biomass burning aerosols determined by proton nuclear magnetic resonance (<sup>1</sup>H-NMR) spectroscopy during the 2008 EUCAARI campaign in the Po Valley (Italy), Atmospheric Chemistry and Physics, 14, 5089-5110, 10.5194/acp-14-5089-2014, 2014.

Paglione, M., Gilardoni, S., Rinaldi, M., Decesari, S., Zanca, N., Sandrini, S., Giulianelli, L., Bacco, D., Ferrari, S., Poluzzi, V., Scotto, F., Trentini, A., Poulain, L., Herrmann, H., Wiedensohler, A., Canonaco, F., Prévôt, A. S. H., Massoli, P., Carbone, C., Facchini, M. C., and Fuzzi, S.: The impact of biomass burning and aqueous-phase processing on air quality: a multi-year source apportionment study in the Po Valley, Italy, Atmospheric Chemistry and Physics, 20, 1233-1254, 10.5194/acp-20-1233-2020, 2020.

Passananti, M., Zapadinsky, E., Zanca, T., Kangasluoma, J., Myllys, N., Rissanen, M. P., Kurten, T., Ehn, M., Attoui, M., and Vehkamaki, H.: How well can we predict cluster fragmentation inside a mass spectrometer?, Chem Commun (Camb), 55, 5946-5949, 10.1039/c9cc02896j, 2019.

Peineke, C., Attoui, M. B., and Schmidt-Ott, A.: Using a glowing wire generator for production of charged, uniformly sized nanoparticles at high concentrations, Journal of Aerosol Science, 37, 1651-1661, 10.1016/j.jaerosci.2006.06.006, 2006.

Peng, J. F., Hu, M., Wang, Z. B., Huang, X. F., Kumar, P., Wu, Z. J., Guo, S., Yue, D. L., Shang, D. J., Zheng, Z., and He, L. Y.: Submicron aerosols at thirteen diversified sites in China: size distribution, new particle formation and corresponding contribution to cloud condensation nuclei production, Atmos. Chem. Phys., 14, 10249-10265, 10.5194/acp-14-10249-2014, 2014.

Rose, C., Sellegri, K., Velarde, F., Moreno, I., Ramonet, M., Weinhold, K., Krejci, R., Ginot, P., Andrade, M., Wiedensohler, A., and Laj, P.: Frequent nucleation events at the high altitude station of Chacaltaya (5240 m a.s.l.), Bolivia, Atmospheric Environment, 102, 18-29, 10.1016/j.atmosenv.2014.11.015, 2015.

Saarikoski, S., Carbone, S., Decesari, S., Giulianelli, L., Angelini, F., Canagaratna, M., Ng, N. L., Trimborn, A., Facchini, M. C., Fuzzi, S., Hillamo, R., and Worsnop, D.: Chemical characterization of springtime submicrometer aerosol in Po Valley, Italy, Atmospheric Chemistry and Physics, 12, 8401-8421, 10.5194/acp-12-8401-2012, 2012.

Schobesberger, S., Junninen, H., Bianchi, F., Lonn, G., Ehn, M., Lehtipalo, K., Dommen, J., Ehrhart, S., Ortega, I. K., Franchin, A., Nieminen, T., Riccobono, F., Hutterli, M., Duplissy, J., Almeida, J., Amorim, A., Breitenlechner, M., Downard, A. J., Dunne, E. M., Flagan, R. C., Kajos, M., Keskinen, H., Kirkby, J., Kupc, A., Kurten, A., Kurten, T., Laaksonen, A., Mathot, S., Onnela, A., Praplan, A. P., Rondo, L., Santos, F. D., Schallhart, S., Schnitzhofer, R., Sipila, M., Tome, A., Tsagkogeorgas, G., Vehkamaki, H., Wimmer, D., Baltensperger, U., Carslaw, K. S., Curtius, J., Hansel, A., Petaja, T., Kulmala, M., Donahue, N. M., and Worsnop, D. R.: Molecular understanding of atmospheric particle formation from sulfuric acid and large oxidized organic molecules, Proc Natl Acad Sci U S A, 110, 17223-17228, 10.1073/pnas.1306973110, 2013.

Schraufnagel, D. E.: The health effects of ultrafine particles, Exp Mol Med, 52, 311-317, 10.1038/s12276-020-0403-3, 2020.
Sebastian, M., Kompalli, S. K., Kumar, V. A., Jose, S., Babu, S. S., Pandithurai, G., Singh, S., Hooda, R. K., Soni, V. K., Pierce, J. R., Vakkari, V., Asmi, E., Westervelt, D. M., Hyvärinen, A.-P., and Kanawade, V. P.: Observations of particle number size distributions and new particle formation in six Indian locations, Atmospheric Chemistry and Physics, 22, 4491-4508, 10.5194/acp-22-4491-2022, 2022.
Shen, J., Bigi, A., Marinoni, A., Lampilahti, J., Kontkanen, J., Ciarelli, G., Putaud, J. P., Nieminen, T., Kulmala, M., Lehtipalo, K., and Bianchi, F.: Emerging Investigator Series: COVID-19 lockdown effects on aerosol particle size distributions in northern Italy, Environ Sci Atmos, 1, 214-227, 10.1039/d1ea00016k, 2021.
Shen, X. J., Sun, J. Y., Zhang, Y. M., Wehner, B., Nowak, A., Tuch, T., Zhang, X. C., Wang, T. T., Zhou, H. G., Zhang, X. L., Dong, F., Birmili, W., and Wiedensohler, A.: First long-term study of particle number size distributions and new particle formation events of regional aerosol in the North China Plain, Atmospheric Chemistry and Physics, 11, 1565-1580, 10.5194/acp-11-1565-2011, 2011.
Simon, M., Dada, L., Heinritzi, M., Scholz, W., Stolzenburg, D., Fischer, L., Wagner, A. C., Kürten, A., Rörup, B., He, X.-C., Almeida, J., Baalbaki, R., Baccarini, A., Bauer, P. S., Beck, L., Bergen, A., Bianchi, F., Bräkling, S., Brilke, S., Caudillo, L., Chen, D., Chu, B., Dias, A., Draper, D. C., Duplissy, J., El-Haddad, I., Finkenzeller, H., Frege, C., Gonzalez-Carracedo, L., Gordon, H., Granzin, M., Hakala, J., Hofbauer, V., Hoyle, C. R., Kim, C., Kong, W., Lamkaddam, H., Lee, C. P., Lehtipalo, K., Leiminger, M., Mai, H., Manninen, H. E., Marie, G., Marten, R., Mentler, B., Molteni, U., Nichman, L., Nie, W., Ojdanic, A., Onnela, A., Partoll, E., Petäjä, T., Pfeifer, J., Philippov, M., Quéléver, L. L. J., Ranjithkumar, A., Rissanen, M. P., Schallhart, S., Schobesberger, S., Schuchmann, S., Shen, J., Sipilä, M., Steiner, G., Stozhkov, Y., Tauber, C., Tham, Y. J., Tomé, A. R., Vazquez-Pufleau, M., Vogel, A. L., Wagner, R., Wang, M., Wang, D. S., Wang, Y., Weber, S. K., Wu, Y., Xiao, M., Yan, C., Ye, P., Ye, Q., Zauner-Wieczorek, M., Zhou, X., Baltensperger, U., Dommen, J., Flagan, R. C., Hansel, A., Kulmala, M., Volkamer, R., Winkler, P. M., Worsnop, D. R., Donahue, N. M., Kirkby, J., and Curtius, J.: Molecular understanding of new-particle formation from <i>α</i>-pinene between −50 and +25 °C, Atmospheric Chemistry and Physics, 20, 9183-9207, 10.5194/acp-20-9183-2020, 2020.
Sipila, M., Sarnela, N., Jokinen, T., Henschel, H., Junninen, H., Kontkanen, J., Richters, S., Kangasluoma, J., Franchin, A., Perakyla, O., Rissanen, M. P., Ehn, M., Vehkamaki, H., Kurten, T., Berndt, T., Petaja, T., Worsnop, D., Ceburnis, D., Kerminen, V. M., Kulmala, M., and O'Dowd, C.: Molecular-scale evidence of aerosol particle formation via sequential addition of HIO3, Nature, 537, 532-534, 10.1038/nature19314, 2016.
Song, Z., Gao, W., Shen, H., Jin, Y., Zhang, C., Luo, H., Pan, L., Yao, B., Zhang, Y., Huo, J., Sun, Y., Yu, D., Chen, H., Chen, J., Duan, Y., Zhao, D., and Xu, J.: Roles of Regional Transport and Vertical Mixing in Aerosol Pollution in Shanghai Over the COVID-19 Lockdown Period Observed Above Urban Canopy, Journal of Geophysical Research: Atmospheres, 128, e2023JD038540, https://doi.org/10.1029/2023JD038540, 2023.
Stolzenburg, D., Fischer, L., Vogel, A. L., Heinritzi, M., Schervish, M., Simon, M., Wagner, A. C., Dada, L., Ahonen, L. R., Amorim, A., Baccarini, A., Bauer, P. S., Baumgartner, B., Bergen, A., Bianchi, F., Breitenlechner, M., Brilke, S., Buenrostro Mazon, S., Chen, D., Dias, A., Draper, D. C., Duplissy, J., El Haddad, I., Finkenzeller, H., Frege, C., Fuchs, C., Garmash, O., Gordon, H., He, X., Helm, J., Hofbauer, V., Hoyle, C. R., Kim, C., Kirkby, J., Kontkanen, J., Kurten, A., Lampilahti, J., Lawler, M., Lehtipalo, K., Leiminger, M., Mai, H., Mathot, S., Mentler, B., Molteni, U., Nie, W., Nieminen, T., Nowak, J. B., Ojdanic, A., Onnela, A., Passananti, M., Petaja, T., Quelever, L. L. J., Rissanen, M. P., Sarnela, N., Schallhart, S., Tauber, C., Tome, A., Wagner, R., Wang, M., Weitz, L., Wimmer, D., Xiao, M., Yan, C., Ye, P., Zha, Q., Baltensperger, U., Curtius, J., Dommen, J., Flagan, R. C., Kulmala, M., Smith, J. N., Worsnop, D. R., Hansel, A., Donahue, N. M., and Winkler, P. M.: Rapid growth of organic aerosol nanoparticles over a wide tropospheric temperature range, Proc Natl Acad Sci U S A, 115, 9122-9127, 10.1073/pnas.1807604115, 2018.

914 Stolzenburg, D., Simon, M., Ranjithkumar, A., Kürten, A., Lehtipalo, K., Gordon, H., Ehrhart, S.,
915 Finkenzeller, H., Pichelstorfer, L., Nieminen, T., He, X.-C., Brilke, S., Xiao, M., Amorim, A., Baalbaki, R.,
916 Baccarini, A., Beck, L., Bräkling, S., Caudillo Murillo, L., Chen, D., Chu, B., Dada, L., Dias, A., Dommen,
917 J., Duplissy, J., El Haddad, I., Fischer, L., Gonzalez Carracedo, L., Heinritzi, M., Kim, C., Koenig, T. K.,
918 Kong, W., Lamkaddam, H., Lee, C. P., Leiminger, M., Li, Z., Makhmutov, V., Manninen, H. E., Marie, G.,
919 Marten, R., Müller, T., Nie, W., Partoll, E., Petäjä, T., Pfeifer, J., Philippov, M., Rissanen, M. P., Rörup,
920 B., Schobesberger, S., Schuchmann, S., Shen, J., Sipilä, M., Steiner, G., Stozhkov, Y., Tauber, C., Tham,
921 Y. J., Tomé, A., Vazquez-Pufleau, M., Wagner, A. C., Wang, M., Wang, Y., Weber, S. K., Wimmer, D.,
922 Wlasits, P. J., Wu, Y., Ye, Q., Zauner-Wieczorek, M., Baltensperger, U., Carslaw, K. S., Curtius, J.,
923 Donahue, N. M., Flagan, R. C., Hansel, A., Kulmala, M., Lelieveld, J., Volkamer, R., Kirkby, J., and Winkler,
924 P. M.: Enhanced growth rate of atmospheric particles from sulfuric acid, Atmospheric Chemistry and
925 Physics, 20, 7359-7372, 10.5194/acp-20-7359-2020, 2020.
926 Ude, S. and de la Mora, J. F.: Molecular monodisperse mobility and mass standards from electrosprays
927 of tetra-alkyl ammonium halides, Journal of Aerosol Science, 36, 1224-1237,
928 https://doi.org/10.1016/j.jaerosci.2005.02.009, 2005.
929 Vana, M., Komsaare, K., Hõrrak, U., Mirme, S., Nieminen, T., Kontkanen, J., Manninen, H. E., Petäjä, T.,
930 Noe, S. M., and Kulmala, M.: Characteristics of new-particle formation at three SMEAR stations, Boreal
931 Environment Research, 2016.
932 Vanhanen, J., Mikkilä, J., Lehtipalo, K., Sipilä, M., Manninen, H. E., Siivola, E., Petäjä, T., and Kulmala,
933 M.: Particle Size Magnifier for Nano-CN Detection, Aerosol Science and Technology, 45, 533-542,
934 10.1080/02786826.2010.547889, 2011.
935 Wang, Z., Wu, Z., Yue, D., Shang, D., Guo, S., Sun, J., Ding, A., Wang, L., Jiang, J., Guo, H., Gao, J., Cheung,
936 H. C., Morawska, L., Keywood, M., and Hu, M.: New particle formation in China: Current knowledge
937 and further directions, Science of The Total Environment, 577, 258-266,
938 10.1016/j.scitotenv.2016.10.177, 2017.
939 Wang, Z. B., Hu, M., Pei, X. Y., Zhang, R. Y., Paasonen, P., Zheng, J., Yue, D. L., Wu, Z. J., Boy, M., and
940 Wiedensohler, A.: Connection of organics to atmospheric new particle formation and growth at an
941 urban site of Beijing, Atmospheric Environment, 103, 7-17, 10.1016/j.atmosenv.2014.11.069, 2015.
942 Wang, Z. B., Hu, M., Sun, J. Y., Wu, Z. J., Yue, D. L., Shen, X. J., Zhang, Y. M., Pei, X. Y., Cheng, Y. F., and
943 Wiedensohler, A.: Characteristics of regional new particle formation in urban and regional background
944 environments in the North China Plain, Atmospheric Chemistry and Physics, 13, 12495-12506,
945 10.5194/acp-13-12495-2013, 2013.
946 Wu, Z., Hu, M., Yue, D., Wehner, B., and Wiedensohler, A.: Evolution of particle number size
947 distribution in an urban atmosphere during episodes of heavy pollution and new particle formation,
948 Science China Earth Sciences, 54, 1772-1778, 10.1007/s11430-011-4227-9, 2011.
949 Wu, Z., Hu, M., Liu, S., Wehner, B., Bauer, S., Ma ßling, A., Wiedensohler, A., Petäjä, T., Dal Maso, M.,
950 and Kulmala, M.: New particle formation in Beijing, China: Statistical analysis of a 1-year data set,
951 Journal of Geophysical Research, 112, 10.1029/2006jd007406, 2007.
952 Xiao, M., Hoyle, C. R., Dada, L., Stolzenburg, D., Kürten, A., Wang, M., Lamkaddam, H., Garmash, O.,
953 Mentler, B., Molteni, U., Baccarini, A., Simon, M., He, X.-C., Lehtipalo, K., Ahonen, L. R., Baalbaki, R.,
954 Bauer, P. S., Beck, L., Bell, D., Bianchi, F., Brilke, S., Chen, D., Chiu, R., Dias, A., Duplissy, J., Finkenzeller,
955 H., Gordon, H., Hofbauer, V., Kim, C., Koenig, T. K., Lampilahti, J., Lee, C. P., Li, Z., Mai, H., Makhmutov,
956 V., Manninen, H. E., Marten, R., Mathot, S., Mauldin, R. L., Nie, W., Onnela, A., Partoll, E., Petäjä, T.,
957 Pfeifer, J., Pospisilova, V., Quéléver, L. L. J., Rissanen, M., Schobesberger, S., Schuchmann, S., Stozhkov,
958 Y., Tauber, C., Tham, Y. J., Tomé, A., Vazquez-Pufleau, M., Wagner, A. C., Wagner, R., Wang, Y., Weitz,
959 L., Wimmer, D., Wu, Y., Yan, C., Ye, P., Ye, Q., Zha, Q., Zhou, X., Amorim, A., Carslaw, K., Curtius, J.,
960 Hansel, A., Volkamer, R., Winkler, P. M., Flagan, R. C., Kulmala, M., Worsnop, D. R., Kirkby, J., Donahue,
961 N. M., Baltensperger, U., El Haddad, I., and Dommen, J.: The driving factors of new particle formation
962 and growth in the polluted boundary layer, Atmospheric Chemistry and Physics, 21, 14275-14291,
963 10.5194/acp-21-14275-2021, 2021.

964 Xiao, S., Wang, M. Y., Yao, L., Kulmala, M., Zhou, B., Yang, X., Chen, J. M., Wang, D. F., Fu, Q. Y.,
965 Worsnop, D. R., and Wang, L.: Strong atmospheric new particle formation in winter in urban Shanghai,
966 China, Atmospheric Chemistry and Physics, 15, 1769-1781, 10.5194/acp-15-1769-2015, 2015.
967 Yan, C., Yin, R., Lu, Y., Dada, L., Yang, D., Fu, Y., Kontkanen, J., Deng, C., Garmash, O., Ruan, J., Baalbaki,
968 R., Schervish, M., Cai, R., Bloss, M., Chan, T., Chen, T., Chen, Q., Chen, X., Chen, Y., Chu, B., Dällenbach,
969 K., Foreback, B., He, X., Heikkinen, L., Jokinen, T., Junninen, H., Kangasluoma, J., Kokkonen, T., Kurppa,
970 M., Lehtipalo, K., Li, H., Li, H., Li, X., Liu, Y., Ma, Q., Paasonen, P., Rantala, P., Pileci, R. E., Rusanen, A.,
971 Sarnela, N., Simonen, P., Wang, S., Wang, W., Wang, Y., Xue, M., Yang, G., Yao, L., Zhou, Y., Kujansuu,
972 J., Petäjä, T., Nie, W., Ma, Y., Ge, M., He, H., Donahue, N. M., Worsnop, D. R., Veli-Matti, K., Wang, L.,
973 Liu, Y., Zheng, J., Kulmala, M., Jiang, J., and Bianchi, F.: The Synergistic Role of Sulfuric Acid, Bases, and
974 Oxidized Organics Governing New-Particle Formation in Beijing, Geophysical Research Letters, 48,
975 10.1029/2020gl091944, 2021.
976 Yan, C., Nie, W., Vogel, A. L., Dada, L., Lehtipalo, K., Stolzenburg, D., Wagner, R., Rissanen, M. P., Xiao,
977 M., Ahonen, L., Fischer, L., Rose, C., Bianchi, F., Gordon, H., Simon, M., Heinritzi, M., Garmash, O.,
978 Roldin, P., Dias, A., Ye, P., Hofbauer, V., Amorim, A., Bauer, P. S., Bergen, A., Bernhammer, A.-K.,
979 Breitenlechner, M., Brilke, S., Buchholz, A., Mazon, S. B., Canagaratna, M. R., Chen, X., Ding, A.,
980 Dommen, J., Draper, D. C., Duplissy, J., Frege, C., Heyn, C., Guida, R., Hakala, J., Heikkinen, L., Hoyle, C.
981 R., Jokinen, T., Kangasluoma, J., Kirkby, J., Kontkanen, J., Kürten, A., Lawler, M. J., Mai, H., Mathot, S.,
982 Mauldin, R. L., Molteni, U., Nichman, L., Nieminen, T., Nowak, J., Ojdanic, A., Onnela, A., Pajunoja, A.,
983 Petäjä, T., Piel, F., Quéléver, L. L. J., Sarnela, N., Schallhart, S., Sengupta, K., Sipilä, M., Tomé, A., Tröstl,
984 J., Väisänen, O., Wagner, A. C., Ylisirniö, A., Zha, Q., Baltensperger, U., Carslaw, K. S., Curtius, J., Flagan,
985 R. C., Hansel, A., Riipinen, I., Smith, J. N., Virtanen, A., Winkler, P. M., Donahue, N. M., Kerminen, V.-
986 M., Kulmala, M., Ehn, M., and Worsnop, D. R.: Size-dependent influence of NO<sub>x</sub> on the
987 growth rates of organic aerosol particles, Science Advances, 6, eaay4945, doi:10.1126/sciadv.aay4945,
988 2020.
989 Yao, L., Wang, M.-Y., Wang, X.-K., Liu, Y.-J., Chen, H.-F., Zheng, J., Nie, W., Ding, A.-J., Geng, F.-H., Wang,
990 D.-F., Chen, J.-M., Worsnop, D. R., and Wang, L.: Detection of atmospheric gaseous amines and amides
991 by a high-resolution time-of-flight chemical ionization mass spectrometer with protonated ethanol
992 reagent ions, Atmospheric Chemistry and Physics, 16, 14527-14543, 10.5194/acp-16-14527-2016,
993 2016.
994 Yao, L., Garmash, O., Bianchi, F., Zheng, J., Yan, C., Kontkanen, J., Junninen, H., Mazon, S. B., Ehn, M.,
995 Paasonen, P., Sipila, M., Wang, M. Y., Wang, X. K., Xiao, S., Chen, H. F., Lu, Y. Q., Zhang, B. W., Wang,
996 D. F., Fu, Q. Y., Geng, F. H., Li, L., Wang, H. L., Qiao, L. P., Yang, X., Chen, J. M., Kerminen, V. M., Petaja,
997 T., Worsnop, D. R., Kulmala, M., and Wang, L.: Atmospheric new particle formation from sulfuric acid
998 and amines in a Chinese megacity, Science, 361, 278-+, 10.1126/science.aao4839, 2018.
999 Yu, H., Zhou, L., Dai, L., Shen, W., Dai, W., Zheng, J., Ma, Y., and Chen, M.: Nucleation and growth of
1000 sub-3 nm particles in the polluted urban atmosphere of a megacity in China, Atmospheric Chemistry
1001 and Physics, 16, 2641-2657, 10.5194/acp-16-2641-2016, 2016.
1002 Yue, D. L., Hu, M., Wang, Z. B., Wen, M. T., Guo, S., Zhong, L. J., Wiedensohler, A., and Zhang, Y. H.:
1003 Comparison of particle number size distributions and new particle formation between the urban and
1004 rural sites in the PRD region, China, Atmospheric Environment, 76, 181-188,
1005 10.1016/j.atmosenv.2012.11.018, 2013.
1006 Zha, Q., Huang, W., Aliaga, D., Peräkylä, O., Heikkinen, L., Koenig, A. M., Wu, C., Enroth, J., Gramlich,
1007 Y., Cai, J., Carbone, S., Hansel, A., Petäjä, T., Kulmala, M., Worsnop, D., Sinclair, V., Krejci, R., Andrade,
1008 M., Mohr, C., and Bianchi, F.: Measurement report: Molecular-level investigation of atmospheric
1009 cluster ions at the tropical high-altitude research station Chacaltaya (5240 m a.s.l.) in the Bolivian
1010 Andes, Atmospheric Chemistry and Physics, 23, 4559-4576, 10.5194/acp-23-4559-2023, 2023a.
1011 Zha, Q., Yan, C., Junninen, H., Riva, M., Sarnela, N., Aalto, J., Quéléver, L., Schallhart, S., Dada, L.,
1012 Heikkinen, L., Peräkylä, O., Zou, J., Rose, C., Wang, Y., Mammarella, I., Katul, G., Vesala, T., Worsnop,
1013 D. R., Kulmala, M., Petäjä, T., Bianchi, F., and Ehn, M.: Vertical characterization of highly oxygenated

molecules (HOMs) below and above a boreal forest canopy, Atmospheric Chemistry and Physics, 18, 17437-17450, 10.5194/acp-18-17437-2018, 2018.
Zha, Q., Aliaga, D., Krejci, R., Sinclair, V., Wu, C., Ciarelli, G., Scholz, W., Heikkinen, L., Partoll, E., Gramlich, Y., Huang, W., Leiminger, M., Enroth, J., Peräkylä, O., Cai, R., Chen, X., Koenig, A. M., Velarde, F., Moreno, I., Petäjä, T., Artaxo, P., Laj, P., Hansel, A., Carbone, S., Kulmala, M., Andrade, M., Worsnop, D., Mohr, C., and Bianchi, F.: Oxidized organic molecules in the tropical free troposphere over Amazonia, National Science Review, 10.1093/nsr/nwad138, 2023b.
Zheng, Y., Chen, Q., Cheng, X., Mohr, C., Cai, J., Huang, W., Shrivastava, M., Ye, P., Fu, P., Shi, X., Ge, Y., Liao, K., Miao, R., Qiu, X., Koenig, T. K., and Chen, S.: Precursors and Pathways Leading to Enhanced Secondary Organic Aerosol Formation during Severe Haze Episodes, Environ Sci Technol, 55, 15680-15693, 10.1021/acs.est.1c04255, 2021.

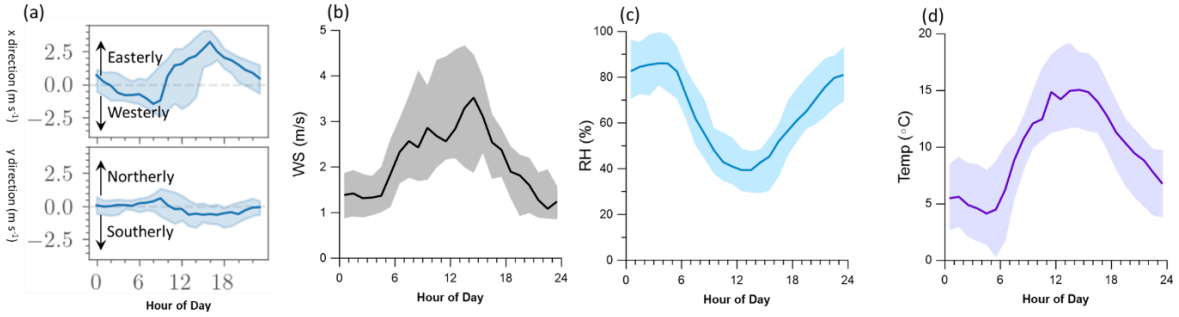


**Figure 1**. The diurnal variations of (a) average wind vectors, (b) wind speed, (c) relative humidity (RH), and (d) temperature.

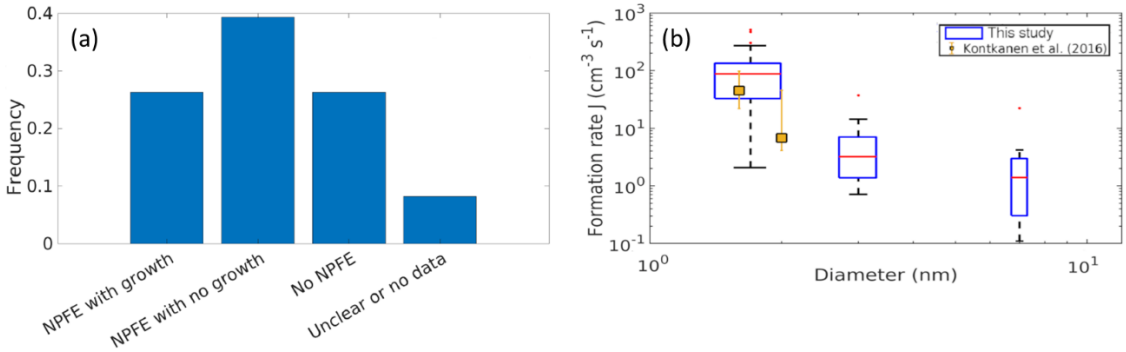


**Figure 2.** (a) The frequency of NPF events with and without growth, of days without NPF, and days with unclear classification or no data during this study, (b) calculated formation rates at 1.7 nm, 3 nm and 7 nm from this study and values reported by Kontkanen et al. 2016 (yellow squares). The red lines are the median values of the maximum formation rates measured during an NPF event, the blue boxes show the values between 25th and 75th percentiles and the black whiskers mark the 5$^{th}$ and 95$^{th}$ percentiles. Red dots are outliers, and the width of the box is proportional to the square root of the number of the *J* values.

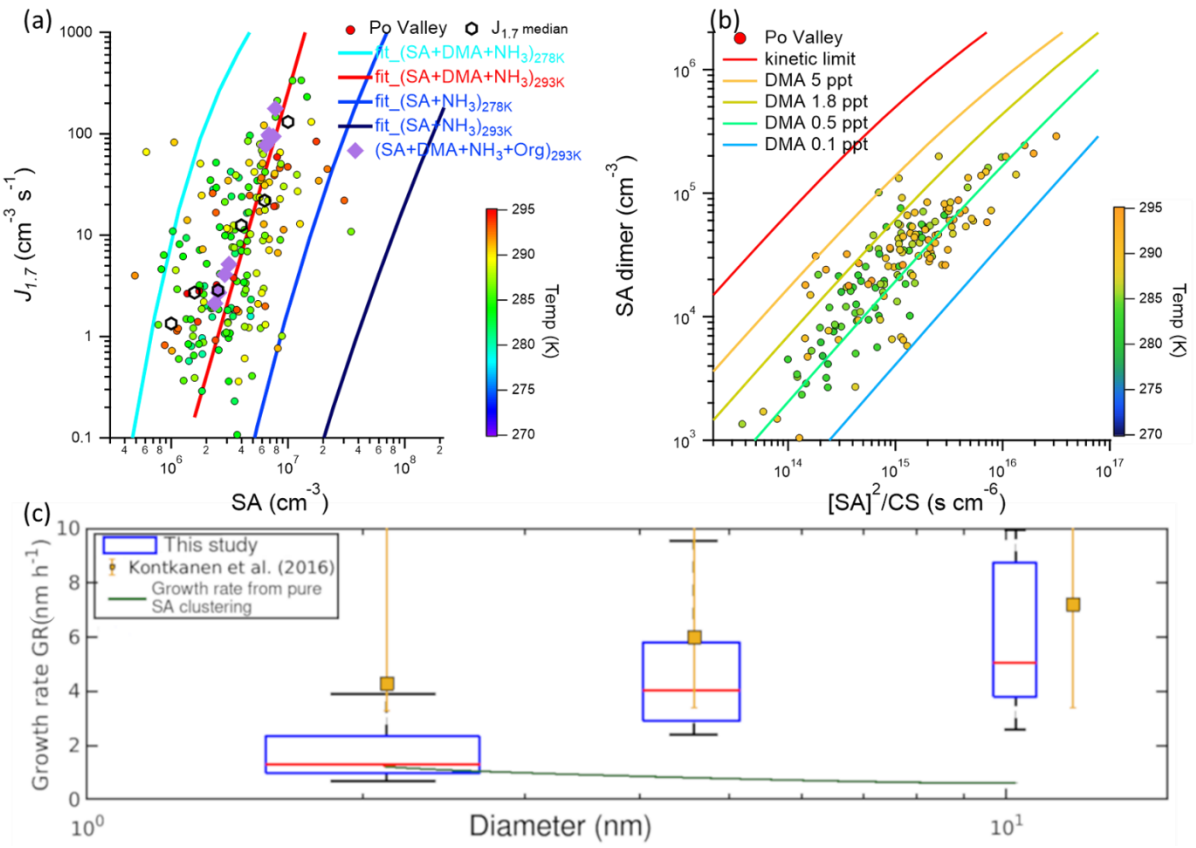


**Figure 3.** (a) The formation rate of 1.7 nm particles ($J_{1.7}$) versus SA concentrations in during springtime in the Po Valley (shown as circles) and experimental results from CLOUD chamber experiments. The solid lines are from fitted results of CLOUD chamber experiments and the black hexagon represented the median values under different SA levels from the ambient measurement, (b) the relationship between sulfuric acid dimer concentration (SA dimer), the square of monomer concentrations $(SA)^2$, and the CS. The lines are from the kinetic model simulations under different DMA levels and the dots are from the measurement. In (a) and (b), the results from the field measurements are from the daytime (10:00 – 14:00 LT) and color-coded by the temperature at the site. The $J_{1.7}$ and corresponding SA concentrations of CLOUD chamber results are from previous literature (Xiao et al., 2021). (c) Calculated growth rates for 1.5 – 3 nm, 3 – 7 nm, and 7 – 15 nm from this study and values reported by Kontkanen et al. (2016, yellow squares). The red horizontal lines are the median values, the blue boxes show the values between 25$^{th}$ and 75$^{th}$ percentiles and the black whiskers mark the 5$^{th}$ and 95$^{th}$ percentiles. The green solid line represents predicted growth rates from pure sulfuric acid without organics condensation (Stolzenburg et al., 2020). The width of the box is proportional to the square root of the number of the GR values.

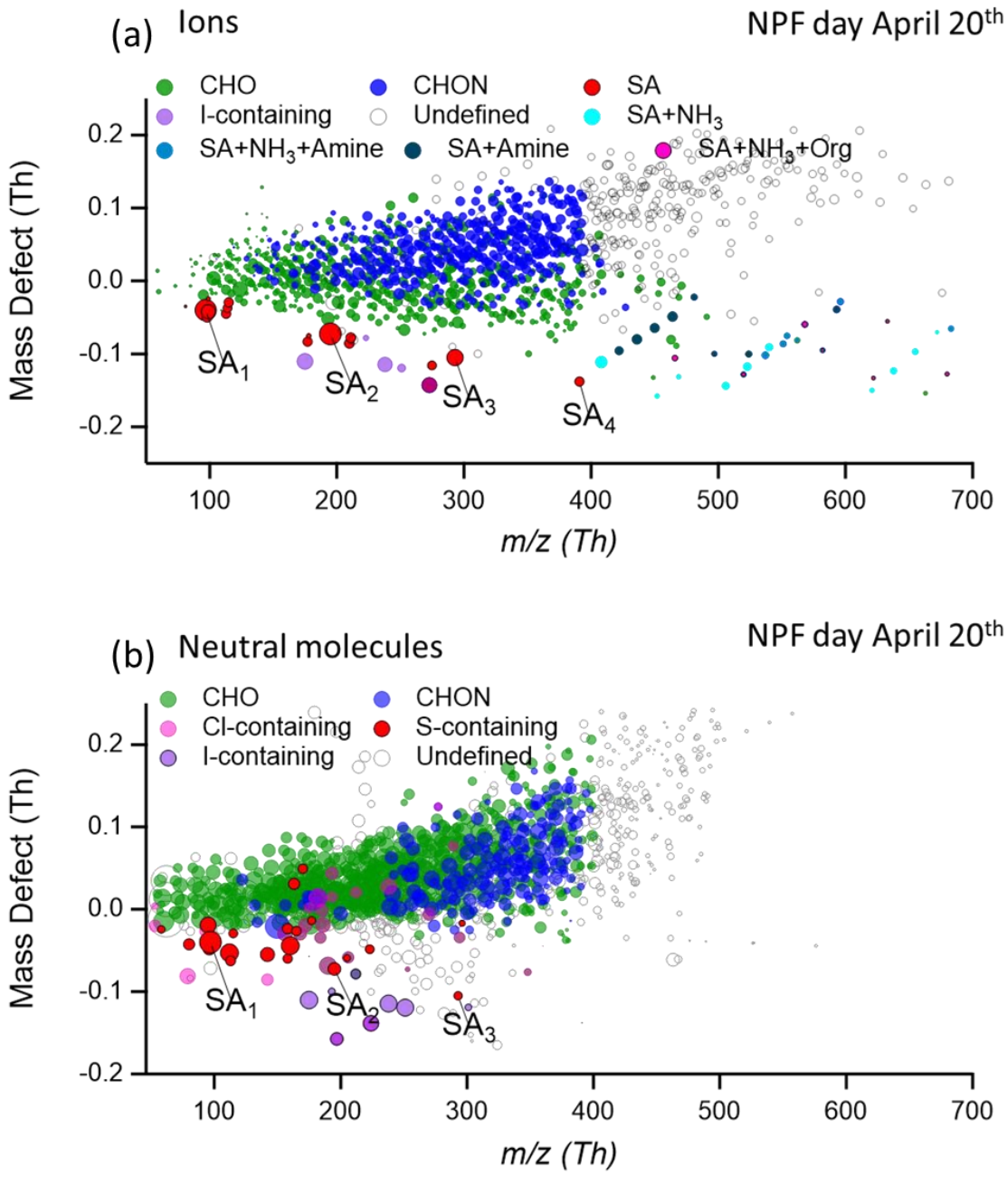


**Figure 4.** Mass defect plots, which represent the difference between compounds' exact mass and nominal mass, for (a) ion clusters and (b) neutral clusters during the NPF period (10:00 − 14:00 LT) of April 20. The size of the dots is proportional to the logarithm of the signal intensity of each cluster.

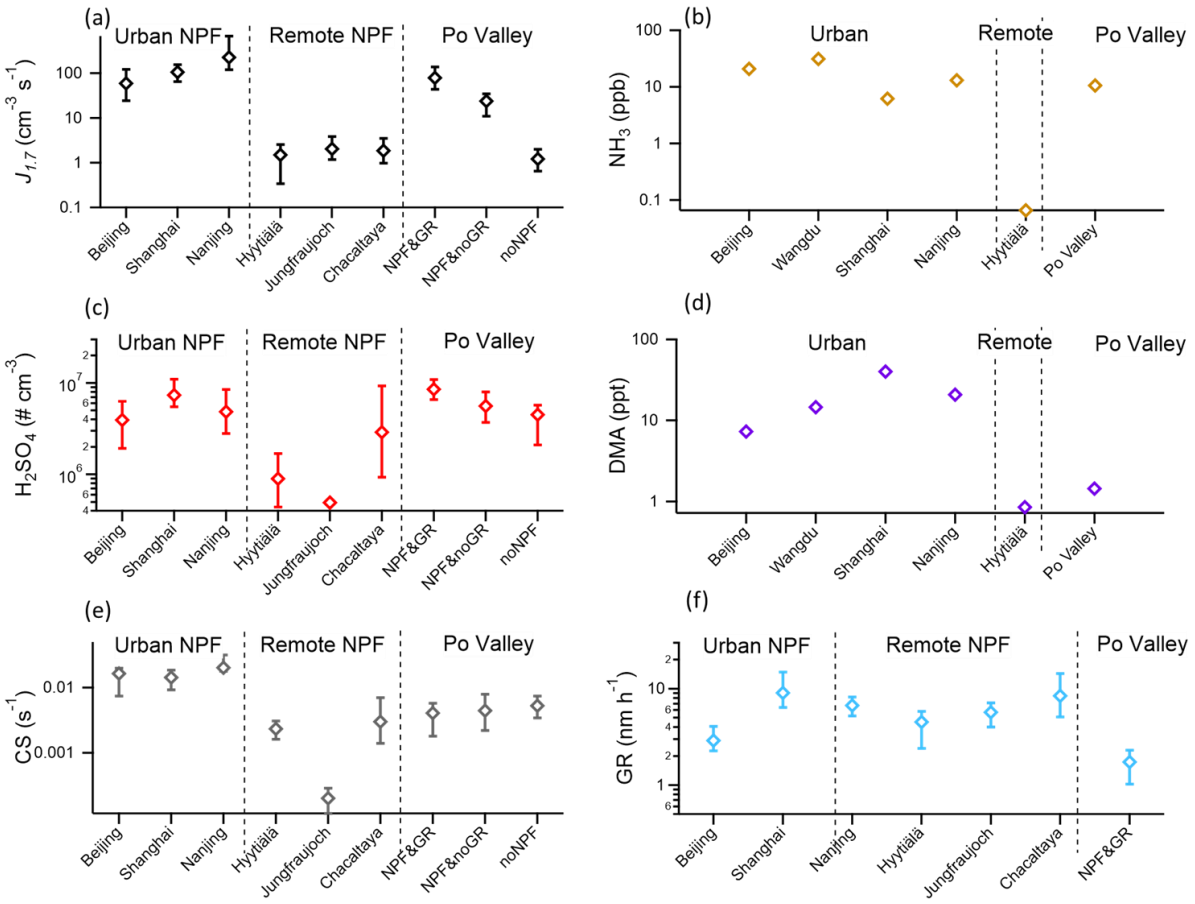


**Figure 5.** Parameters and gaseous precursors related to NPF in the Po Valley and other environments. (a) formation rate of sub-2 nm particles, (b) the atmospheric $NH_3$ concentrations, (c) SA concentrations, (d) DMA concentrations, (e) CS levels, and (f) growth rate in different environments. The diamond dots represent the median values, and the error bars represent the 25$^{th}$ and 75$^{th}$ percentiles. For the Po Valley data, the formation rates, growth rates, SA concentrations and CS data were selected for 10:00 – 14:00 LT. The formation rates, growth rates, SA concentrations and CS during NPF in Beijing, Shanghai, Hyytiälä, Jungfraujoch and Chacaltaya are from Deng et al. (2020). The GR calculation range varies for different sites. Beijing ($GR_{7–15,}$ (Deng et al., 2020)), Shanghai ($GR_{7–25,}$ (Yao et al., 2018)), Nanjing ($GR_{3–20,}$ (Yu et al., 2016)), Hyytiälä ($GR_{3–20,}$ (Vana et al., 2016)), Jungfraujoch ($GR_{7–20,}$ (Boulon et al., 2010)), Chacaltaya ($GR_{7–20,}$ (Rose et al., 2015)), and Po Valley ($GR_{7–15,}$ this study) are used for comparison. The $NH_3$ and DMA concentrations are from literature, which is listed in the Table S1. Half of the limit of detection (LOD) of DMA concentrations in Hyytiälä was applied in panel d (Hemmilä et al., 2018). DMA concentrations in Po Valley was not presented since it is not quantified in this study.